Inorganic Chemistry

Article

pubs.acs.org/IC

Synthesis, Lanthanide Coordination Chemistry, and Liquid–Liquid Extraction Performance of CMPO-Decorated Pyridine and Pyridine *N*-Oxide Platforms

Daniel Rosario-Amorin,[†] Sabrina Ouizem,[†] Diane A. Dickie,[†] Yufeng Wen,[†] Robert T. Paine,*[,†] Jian Gao,[†] John K. Grey,[†] Ana de Bettencourt-Dias,[‡] Benjamin P. Hay,[§] and Lætitia H. Delmau[§]

[†]Department of Chemistry and Chemical Biology, University of New Mexico, Albuquerque, New Mexico 87131, United States

[‡]Department of Chemistry, University of Nevada, Reno, Nevada 89557, United States

[§]Chemical Sciences Division, Oak Ridge National Laboratory, P.O. Box 2008, Oak Ridge, Tennessee 37831, United States

Supporting Information

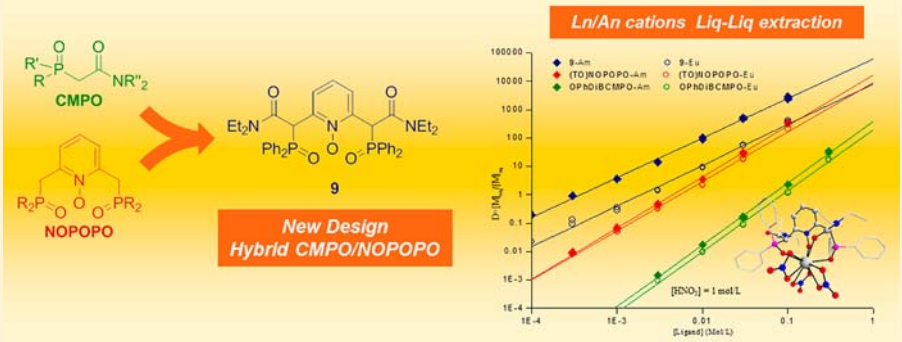

ABSTRACT: Syntheses for a set of new ligands containing one or two carbamoylmethylphosphine oxide (CMPO) fragments appended to pyridine and pyridine *N*-oxide platforms are described. Molecular mechanics analyses for gas phase lanthanide–ligand interactions for the pyridine *N*-oxides indicate that the trifunctional NOPOCO molecules, 2-{[$Ph_2P(O)$][$C(O)NEt_2$]-C(H)}C_5H_4NO (**7**) and 2-{[$Ph_2P(O)$][$C(O)NEt_2$]$CHCH_2$}C_5H_4NO (**8**), and pentafunctional NOPOP′O′COC′O′ molecules, 2,6-{[$Ph_2P(O)$][$C(O)NEt_2$]C(H)}$_2C_5H_3NO$ (**9**) and 2,6-{[$Ph_2P(O)$][$C(O)NEt_2$]$CHCH_2$}$_2C_5H_3NO$ (**10**), should be able to adopt, with minimal strain, tridentate and pentadentate chelate structures, respectively. As a test of these predictions, selected lanthanide coordination chemistry of the *N*-oxide derivatives was explored. Crystal structure analyses reveal the formation of a tridentate NOPOCO chelate structure for a 1:1 Pr(III) complex containing **7** while **8** adopts a mixed bidentate/bridging monodentate POCO/NO binding mode with Pr(III). Tridentate and tetradentate chelate structures are obtained for several 1:1 complexes of **9** while a pentadentate chelate structure is observed with **10**. Emission spectroscopy for one complex, [Eu(**9**)$(NO_3)_3$], in methanol, shows that the Eu(III) ion resides in a low-symmetry site. Lifetime measurements for methanol and deuterated methanol solutions indicate the presence of four methanol molecules in the inner coordination sphere of the metal ion, in addition to the ligand, with the nitrate anions most likely dissociated. The solvent extraction performance of **7**–**10** in 1,2-dichloroethane for Eu(III) and Am(III) in nitric acid solutions was analyzed and compared with the performance of 2,6-bis(di-*n*-octylphosphinoylmethyl)pyridine *N*-oxide (TONOPOP′O′) and *n*-octyl(phenyl)-*N*,*N*-diisobutylcarbamoylmethylphosphine oxide (OPhDiBCMPO) measured under identical conditions.

INTRODUCTION

The development of multifunctional ligands as efficient and selective solvent extraction reagents for inherently difficult f-element ion separations continues to be an important research objective, and many of the fundamental challenges central to extractant design and assembly have been thoroughly summarized.[1−7] Due to the unique coordination properties of the relatively hard f-element ions,[8] only a small number of donor group types have been successfully employed in extractant designs for these ions. Foremost among these are neutral and acidic organophosphorus compounds,[1,2,9,10] and examples of these compounds serve as critical components in large-scale TALSPEAK,[1,2,11] PUREX,[1,2,12] and TRUEX[1,2,13] solvent extraction processes. Nonetheless, there remain limitations with each process that stimulate continued efforts to derive improved extractant systems. This includes development of additional neutral carbamoylmethylphosphine oxide (CMPO) ligands, $RR'P(O)CH_2C(O)NR''_2$, **1**, for general f-element ion partitioning from high-level nuclear waste

Received: November 19, 2012
Published: March 5, 2013

 © 2013 American Chemical Society

solutions, as well as phosphorus-free malonamide-based extractants that are used in the DIAMEX process[2d,3,5,6b,14,15] and bis-triazinyl pyridine-based extractants employed in SANEX and GAMEX processes[2e,3,5,7] for difficult An(III)/Ln(III) group separations.

The known CMPO ligands, in particular, display fundamentally interesting properties. Under typical ligand-loaded biphasic solvent extraction process conditions, they are known to form stable lanthanide (Ln) and actinide (An) ion complexes in the organic phase even in the presence of strong mineral acids, e.g., HNO_3 and HCl. Furthermore, extraction efficiencies unexpectedly increase with increasing acid concentration. Ligand dependency analyses for Ln(III), An(III), and An(IV) cations indicate formation of organic phase soluble complexes containing two to four CMPO ligands depending upon the specific metal ion and the organic diluent. In the case of Am(III) in nitric acid solutions, the extraction complex that is transferred to the organic phase is proposed to be $[Am(CMPO)_3(NO_3)_3]\cdot 3HNO_3$.[16] Solution infrared and NMR spectroscopic data suggest that the CMPO ligands bind to Am(III) in a monodentate mode through the phosphine oxide, O_P, atoms.[17] The three nitrate anions probably reside in the inner coordination sphere, bonded in a bidentate fashion, and the coextracted nitric acid molecules are likely coordinated with the amide carbonyl, O_C, atoms of the CMPO ligands. In contrast, crystal structure analyses for several isolated lanthanide−CMPO complexes, as well as for related lanthanide−carbamoylmethylphosphonate (CMP), $(RO)_2P(O)CH_2C(O)NR'_2$, complexes, typically reveal solid-state structures containing *two* CMPO or CMP ligands and three nitrate anions in the inner coordination sphere. For early lanthanide ions, the CMPO or CMP ligands are bonded in a bidentate, O_PO_C manner while for late lanthanides the CMPO or CMP ligands are bonded in a monodentate mode through the O_P atoms.[18] In the latter complexes, the amide carbonyl O_C atoms are found to be hydrogen bonded with an inner sphere, lanthanide bound, water molecule. In these cases, the three nitrate counterions reside in the inner coordination sphere bound in a bidentate mode. More recently, Odinets and coworkers[19] have also reported the successful isolation and structural characterization of a 3:1 CMPO:Pr(III) complex in which the CMPO ligands are all bonded in a bidentate, O_PO_C manner. The observed structural differences between the solution and solid phase complexes are not unexpected given the competing coordination features present in these systems. Indeed, subsequent detailed quantum mechanical studies of lanthanide−CMPO interactions confirm that, even in the gas phase, there is a sensitive balance of factors responsible for selection of the CMPO (CMP) binding condition.[20] In condensed solution and solid-state phases, the picture is expected to be even more complicated.

These observations, as well as general coordination chemistry principles[8] and molecular mechanics (MM) computational analyses with other donor ligand systems,[21] suggest that improved extraction performance might be realized by preorganization of two or more CMPO or CMP fragments on a central lipophilic platform. Indeed, several groups have explored attachment of CMPO fragments to C_3-symmetric alkyl,[22−26] 1,3,5-trialkyl benzene,[25] C_3-symmetric amine,[26] upper and lower rim-substituted calixarene,[27] and resorcinarene[28] platforms. In each case, the platform attachment linkage involves the amide N-atom of the CMPO fragment. Although the precise compositions and structures of the resulting extraction complexes remain somewhat unclear,[27d,e,29] the preorganized ligands with two, three, and four CMPO fragments display much improved extractant efficiencies and, in some cases, enhanced selectivity performance compared with the parent CMPO. For example, the wide-rim substituted calix[4]arene, **2**, with four CMPO fragments, produces distribution ratios, $D = [M_o]/[M_{aq}]$, depending upon specific conditions, similar to those recorded with solutions that are ∼100 times more concentrated in the parent CMPO.[27a]

During the maturation of the CMPO family of extractants, our group also explored additional families of multifunctional ligands derived by decoration of pyridine platforms. These ligands are illustrated by the general structures **3**−**6** that carry pendent phosphine oxide ($X = P(O)R_2$),[30] phosphonate ($X = P(O)(OR)_2$),[30] methyl phosphine oxide ($X = CH_2P(O)R_2$),[31] and methyl phosphonate ($X = CH_2P(O)(OR)_2$)[31] donor group substituents. The NPO, **3**, and NPOP′O′, **4**, ligands are easily obtained in good yields and high purity, and they form monodentate or bidentate O_P-bonded coordination complexes with Ln(III) ions. In no case, under the conditions utilized, is the pyridine N-atom observed to bond to an f-element cation. With only two exceptions, the corresponding pyridine *N*-oxide NOPO, **5**, and NOPOP′O′, **6**, ligands also are obtained in good yields and high purity. The exceptions appear in attempts to prepare the NOPOP′O′ ligands with $X = P(O)R_2$ and $P(O)(OR)_2$. Here, oxidative ring degradation reactions compete with N-oxidation. The NOPO and NOPOP′O′ ligands form stable coordination complexes with Ln(III), Th(IV), Pu(IV), and U(VI) ions, and X-ray diffraction analyses indicate that the ligands bond to the f-element ions as bidentate O_NO_P and tridentate $O_NO_PO'_{P'}$ chelates, respectively.[30,31] The extraction performance of one NOPO derivative **5**, with $X = P(O)(OHx)_2$ in $CHCl_3$, toward Ce(III), Eu(III), and Yb(III) in aqueous nitric acid solutions, is relatively unremarkable.[32] Most notably, the *D* values *decrease* significantly with increasing acid concentration as expected if nitric acid competes effectively for binding with the ligand. However, despite the need to form larger seven-membered chelate rings, toluene solutions of a derivative of **5** with $X = CH_2P(O)Ph_2$ provide efficient extractions at all acid concentrations ($[HNO_3] = 10^{-2}$ M to 6 M). In addition, the *D* values *increase* with increasing nitric acid concentration between $[HNO_3] = 10^{-2}$ M and 1 M before decreasing.[33] Although the *N*-oxides **6**, with $X = P(O)R_2$ and $P(O)(OR)_2$, are not available for extraction analysis, the extraction performance of methyl phosphine oxides **6** ($X = -CH_2P(O)R_2$) have proven to be especially interesting. Initial survey extractions of Eu(III) and Am(III) in HNO_3 with **6** ($X = CH_2P(O)Ph_2$) in $CHCl_3$ showed that, similar to the CMPO ligands, the *D* values for this NOPOP′O′ molecule *increase* by more than two decades with increasing acid concentration. Between $[HNO_3] = 0.5$−1.0 M, the *D* values are similar to those for equivalent concentrations of CMPO (R = *n*-octyl, R′ = phenyl, R″ = *i*-Bu) while at higher nitric acid concentrations the *D* values for NOPOP′O′ are greater. A further contrast between the two ligand families is found in the ligand dependency analyses. Recall that the CMPO ligand dependency for Am(III) extractions from nitric acid solutions is consistent with the presence of three molecules of CMPO in the extraction complex. However, for NOPOP′O′, the slope analysis indicates that two molecules of the ligand are present in the extraction complex. This observation parallels the stoichiometry found in solid state structures. These results led to more detailed comparative studies of the extraction of

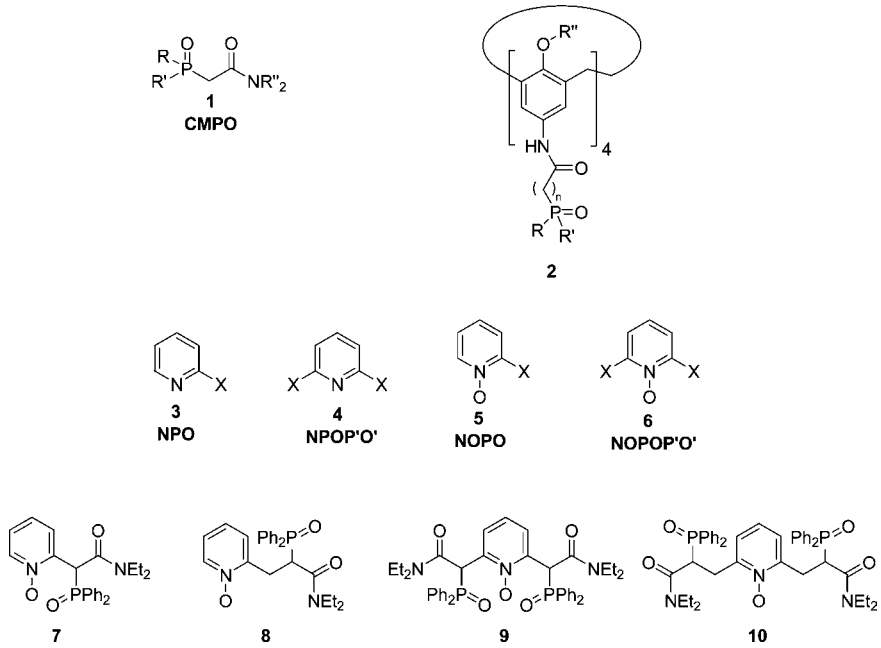

Eu(III) and Am(III) in HNO_3 solutions by toluene and dodecane solutions of **6** (X = $CH_2P(O)(2\text{-ethylhexyl})_2$),[34] and most recently of Eu(III), Am(III), U(VI), Th(IV), Pu(IV), and Np(V) extractions with toluene solution of **6** (X = $CH_2P(O)(n\text{-octyl})_2$).[35] In each case, the NOPOP′O′ derivatives display improved efficiency over CMPO and additional comparative studies continue.

The interesting coordination chemistry and favorable extraction performance displayed by the NOPO and NOPOP′O′ ligands led us to consider potential marriages between these fragments and the CMPO fragment. Of course, there are several options available for incorporating both functionalities into hybrid ligand structures. In this Article, we describe the syntheses, selected lanthanide coordination chemistry, and initial extraction analyses for a set of new hybrid ligands, **7**−**10**, wherein the NOPO/CMPO and NOPOPO/CMPO linkages are made through the methyl carbon atom of the CMPO. Ligands involving attachment through the amide N-atom will be reported separately.

■ EXPERIMENTAL SECTION

General Information. Organic reagents (Aldrich Chemical Co) and metal nitrates (Ventron) were used as received, and organic solvents (VWR) were dried and distilled by standard methods. Reactions were performed under dry nitrogen unless specified otherwise. Infrared spectra were recorded on a Bruker Tensor 27 benchtop spectrometer. Solution NMR spectra were measured with JEOL-GSX400, Bruker FX-250, and Avance-300 and -500 multinuclear spectrometers using Me_4Si (^1H, ^{13}C) and 85% H_3PO_4 (^{31}P) as external standards. Downfield shifts from the reference resonances were given +δ values.[36] Mass spectra for the ligands were obtained from the UNM Mass Spectrometry Center by using electrospray ionization (ESI) with a Waters/Micromass mass spectrometer operating in the positive ion mode. Mass spectra (ESI) for one lanthanide complex, [Eu(**9**)-$(NO_3)_3$], were recorded at UNR with an Agilent Technologies 6230 TOF mass spectrometer in positive ion mode. In the latter case, the sample was previously dissolved in deuterated methanol for photophysical characterization. Consequently, deuterium partially substitutes for hydrogen atoms in some of the observed peaks. Elemental analyses were performed by Galbraith Laboratories.

Ligand Syntheses. *2-(Diphenyl-N,N-diethylcarbamoylmethylphosphine oxide)pyridine (**7**$_N$).* A solution of *n*-BuLi (1.6 M in hexane, 10.7 mL, 17 mmol) was added dropwise, under nitrogen (23 °C, 40 min), to a vigorously stirred solution of 2-(diphenylphosphinoylmethyl)pyridine *P*-oxide[31a,37] (5.02 g, 17 mmol) in dry toluene (90 mL, 23 °C). Following addition of the reagents, a clear, pale red solution was obtained which was heated and stirred (65−70 °C, 1 h). The reaction mixture was then cooled (−40 °C), and diethylcarbamoyl chloride (2.2 mL, 17 mmol) in toluene (10 mL) was added dropwise (30 min, 23 °C) with stirring. The temperature of the mixture was slowly increased, held at 80 °C (1 h), and then cooled and stirred (23 °C, 12 h). The resulting yellow suspension was poured into an ice bath (100 g), and the phases were separated. The aqueous layer was extracted with $CHCl_3$ (2 × 50 mL), and the combined organic phases were washed with water (50 mL). The organic phase was dried (4 Å molecular sieves) and filtered, and the volatiles were removed by vacuum evaporation. The weakly brown residue was triturated with Et_2O (3 × 25 mL) and pentane leaving a white powder, 7_N: yield 3.42 g, 51%; mp 158−160 °C. The compound is soluble in $CHCl_3$, CH_2Cl_2, MeOH, and EtOH, slightly soluble in benzene and acetone, and insoluble in toluene, pentane, and Et_2O. $^{31}P\{^1H\}$ NMR (121.5 MHz, $CDCl_3$): δ 29.5. ^1H NMR (300 MHz, $CDCl_3$): δ 8.41 (d, J_{HH} = 4.2 Hz, 1H, H_1), 7.95−7.70 (m, 5H, $H_{4,11,11'}$), 7.57−7.35 (m, 7H, $H_{3,12,12',13,13'}$), 7.02−6.95 (t, J_{HH} = 5.1 Hz, 1H, H_2), 5.31 (d, J_{HP} = 13.2 Hz, 1H, H_6), 3.41−3.01 (m, 4H, $H_{8,8'}$), 0.98 (t, J_{HH} = 7.1 Hz, 3H, H_9), 0.90 (t, J_{HH} = 7.1 Hz, 3H, $H_{9'}$). $^{13}C\{^1H\}$ NMR (75.5 MHz, $CDCl_3$): δ 166.11 (C_7), 152.60 (d, J_{CP} = 5.7 Hz, C_5), 149.07 (C_1), 136.52 (C_3), 132.21 (d, J_{CP} = 9.4 Hz, C_{11}), 131.93 (d, J_{CP} = 101.7 Hz, $C_{10,10'}$), 131.89 (d, J_{CP} = 9.3 Hz, $C_{11'}$), 131.83 ($C_{13,13'}$), 128.21 (d, J_{CP} = 12.1 Hz, $C_{12,12'}$), 125.33 (d, J_{CP} = 3.0 Hz, C_4), 122.60 (C_2), 56.28 (d, J_{CP} = 64.5 Hz, C_6), 43.04 (C_8), 40.90 ($C_{8'}$), 14.53 (C_9), 12.70 ($C_{9'}$). FTIR (KBr, cm^{-1}): 3054, 2978, 1634 ($\nu_{C=O}$), 1435, 1190 ($\nu_{P=O}$), 1117. HRMS (ESI) *m/z* (%): 393.1737 (100) [M + H^+]. $C_{23}H_{26}N_2O_2P$ requires 393.1732; 415.1560 (23) [M + Na^+]. $C_{23}H_{25}N_2O_2PNa$ requires 415.1551.

*2-(Diphenyl-N,N-diethylcarbamoylmethylphosphine oxide)-pyridine N-Oxide (**7**).* Method A is described here. A sample of 7_N (2.3 g, 5.87 mmol) was dissolved in glacial acetic acid (10 mL) and combined with a solution of H_2O_2 (30%, 3.3 mL, 29 mmol). The mixture was stirred (23 °C, 4 d), and then the volatiles were removed by vacuum evaporation. The remaining white residue was dissolved in $CHCl_3$ (50 mL) and washed with water (3 × 25 mL). The combined aqueous wash solutions were extracted with $CHCl_3$ (2 × 25 mL) and the combined organic phases dried (4 Å molecular sieves). The organic phase was vacuum evaporated leaving a white solid (**7**): yield 1.83 g, 76%. Method B follows here. To a solution of 7_N (2.0 g, 5.1 mmol) in dry CH_2Cl_2 (10 mL) was slowly added *m*-chloroperox-

ybenzoic acid (77 wt %, 3.77 g, 15.3 mmol). The mixture was stirred (23 °C, 12 h) and the resulting mixture diluted with additional CH_2Cl_2 (90 mL) and washed with aqueous NaOH (2 N, 3 × 25 mL) and distilled water (2 × 25 mL). The organic phase was dried (anhydr $MgSO_4$) and filtered, and the volatiles were removed by vacuum evaporation, leaving a white powder, **7**: yield 1.5 g, 72%; mp 134−138 °C. The compound is soluble in $CHCl_3$, CH_2Cl_2, MeOH, and EtOH, slightly soluble in xylenes, benzene, and acetone, and insoluble in Et_2O and heptane. $^{31}P\{^1H\}$ NMR (121.5 MHz, $CDCl_3$): δ 30.4. In d_4-MeOH: δ 31.6. ^1H NMR (300 MHz, $CDCl_3$): δ 8.34 (d, J_{HH} = 7.8 Hz, 1H, H_1), 8.12 (d, J_{HH} = 6.3 Hz, 1H, H_4), 7.92−7.78 (m, 4H, $H_{11,11'}$), 7.54−7.41 (m, 6H, $H_{12,12',13,13'}$), 7.21−7.07 (m, 2H, $H_{2,3}$), 6.67 (d, J_{HP} = 8.6 Hz, 1H, H_6), 3.48−3.37 (dq, J_{HH} = 7.0 Hz, 1H, H_8), 3.22 (q, J_{HH} = 7.1 Hz, 2H, $H_{8'}$), 3.04−2.93 (dq, J_{HH} = 7.0 Hz, 1H, H_8), 0.97 (t, J_{HH} = 7.1 Hz, 3H, H_9), 0.87 (t, J_{HH} = 7.1 Hz, 3H, $H_{9'}$). $^{13}C\{^1H\}$ NMR (75.5 MHz, $CDCl_3$): δ 164.27 (d, J_{CP} = 3.4 Hz, C_7), 143.80 (C_5), 138.49 (C_1), 132.35 (C_3), 131.68 (d, J_{CP} = 9.8 Hz, C_{11}), 131.34 (d, J_{CP} = 9.8 Hz, $C_{11'}$), 130.86 (d, J_{CP} = 104.1 Hz, $C_{10,10'}$), 129.85 (C_{13}), 129.80 ($C_{13'}$), 128.66 (d, J_{CP} = 12.0 Hz, C_{12}), 128.63 (d, J_{CP} = 12.0 Hz, $C_{12'}$), 125.83 (C_4), 124.73 (C_2), 42.98 (C_8), 41.38 (d, J_{CP} = 63.8 Hz, C_6), 41.09 ($C_{8'}$), 14.09 (C_9), 12.65 ($C_{9'}$). FTIR (KBr, cm^{-1}): 3055, 2970, 2933, 2874, 1638 ($\nu_{C=O}$), 1589, 1485, 1435, 1283, 1265 (ν_{N-O}), 1205, 1192 ($\nu_{P=O}$), 1117, 1099, 1072, 995, 951, 916, 841, 773, 752, 729, 702, 561, 550, 513. HRMS (ESI) m/z (%): 409.1687 (100) [M + H^+]. $C_{23}H_{26}N_2O_3P$ requires 409.1681; 431.1500 (18) [M + Na^+]. $C_{23}H_{25}N_2O_3PNa$ requires 431.1501. Anal. Calcd for $C_{23}H_{25}N_2O_3P$: C 67.64, H 6.17, N 6.86. Found C 67.37, H 6.30, N 6.65.

*2-[(Diphenyl-N,N-diethylcarbamoylmethylphosphine oxide)-methyl]pyridine (**8**$_N$).* A solution of *n*-BuLi (1.6 M in hexane, 62.8 mL, 0.10 mol) was added dropwise (40 min), under nitrogen, to a vigorously stirred slurry of diphenyl-*N,N*-diethylcarbamoylmethylphosphine oxide[38] (31.63 g, 0.10 mol) in toluene (300 mL, 23 °C). Following addition of the reagents, a clear, pale red solution was obtained which was heated (80−90 °C, 2 h). The resulting dark red solution was cooled (23 °C) and transferred dropwise (1 h) into a vigorously stirred solution of 2-(chloromethyl)pyridine[31a] (12.8 g, 0.10 mol) in toluene (100 mL, 23 °C). The resulting mixture was stirred and heated (90 °C, 12 h), and then cooled (23 °C). A yellow solid formed that contained the product and LiCl. The solid was collected by filtration under nitrogen and washed with water (100 mL) and the remaining solid dissolved in $CHCl_3$ (100 mL). The aqueous wash solution was extracted with $CHCl_3$ (2 × 50 mL), and the combined organic phases were washed with water (3 × 25 mL) and then dried (4 Å molecular sieves). The organic phase was recovered by filtration and vacuum evaporated leaving a sticky, pale yellow residue that was washed with diethyl ether and vacuum-dried leaving a bone white solid (**8**$_N$): yield: 20.2 g, 50%; mp 116−118 °C. The product is soluble in $CHCl_3$, CH_2Cl_2, EtOH, MeOH and insoluble in toluene, hexane and Et_2O. $^{31}P\{^1H\}$ NMR (121.5 MHz, $CDCl_3$): δ 31.0. ^1H NMR (300 MHz, $CDCl_3$): δ 8.38 (d, J_{HH} = 4.1 Hz, 1H, H_1), 8.13 (dd, J_{HH} = 8.1 Hz, 2H, H_{12}), 7.83 (dd, J_{HH} = 8.1 Hz, 2H, $H_{12'}$), 7.45−7.37 (m, 7H, $H_{3,13,13',14,14'}$), 7.02−6.95 (m, 2H, $H_{2,4}$), 4.35 (t, J_{HP} = 12.6 Hz, 1H, H_7), 3.49−3.39 (m, 1H, H_9), 3.25−3.00 (m, 4H, $H_{6,9'}$), 2.78−2.66 (m, 1H, H_9), 0.71 (t, J_{HH} = 7.1 Hz, 3H, H_{10}), 0.66 (t, J_{HH} = 7.1 Hz, 3H, $H_{10'}$). $^{13}C\{^1H\}$ NMR (75.5 MHz, $CDCl_3$): δ 167.60 (C_8), 158.50 (d, J_{CP} = 14.2 Hz, C_5), 148.93 (C_1), 136.06 (C_3), 132.08 (d, J_{CP} = 9.0 Hz, C_{12}), 131.85 ($C_{14,14'}$), 131.79 (d, J_{CP} = 9.0 Hz, $C_{12'}$), 131.29 (d, J_{CP} = 84.3 Hz, $C_{11,11'}$), 128.41 (d, J_{CP} = 12.1 Hz, C_{13}), 128.21 (d, J_{CP} = 12.1 Hz, $C_{13'}$), 123.73 (C_4), 121.47 (C_2), 45.58 (d, J_{CP} = 61.7 Hz, C_7), 42.42 (C_9), 40.67 ($C_{9'}$), 36.43 (C_6), 13.47 (C_{10}), 12.38 ($C_{10'}$). FTIR (KBr, cm^{-1}): 3059, 2974, 2931, 1634 ($\nu_{C=O}$), 1589, 1435, 1317, 1192 ($\nu_{P=O}$), 1121, 748, 700, 521. HRMS (ESI) m/z (%): 407.1888 (100) [M + H^+]. $C_{24}H_{28}N_2O_2P$ requires 407.1888; 429.1710 (48) [M + Na^+]. $C_{24}H_{27}N_2O_2PNa$ requires 429.1708.

*2-[(Diphenyl-N,N-diethylcarbamoylmethylphosphine oxide)-methyl]pyridine N-Oxide (**8**).* A sample of **8**$_N$ (19.5 g, 48 mmol) was dissolved in glacial acetic acid (60 mL), H_2O_2 (30%, 27.2 mL, 270 mmol) was added, and the mixture was stirred (23 °C, 4 d). The resulting solution was vacuum evaporated and the residue dissolved in $CHCl_3$ (100 mL) and washed with water (3 × 25 mL). The combined aqueous phases were extracted with $CHCl_3$ (2 × 25 mL) and the combined organic phases dried (4 Å molecular sieves). The solution was filtered and the filtrate vacuum evaporated leaving a white solid (**8**): yield 12.4 g, 61%; mp 146−147 °C. The compound is soluble in $CHCl_3$, CH_2Cl_2, MeOH, and EtOH, slightly soluble in xylenes and benzene, and insoluble in Et_2O and pentane. $^{31}P\{^1H\}$ NMR (121.5 MHz, $CDCl_3$): δ 32.0. In d_4-MeOH: δ 35.4. ^1H NMR (300 MHz, $CDCl_3$): δ 7.99 (d, J_{HH} = 5.7 Hz, 1H, H_1), 7.86−7.73 (m, 4H, $H_{12,12'}$), 7.41−7.32 (m, 6H, $H_{13,13',14,14'}$), 7.12 (dd, J_{HH} = 7.5 Hz, 1H, H_3), 6.99−6.95 (m, 2H, $H_{2,4}$), 4.83−4.76 (m, 1H, H_7), 3.41−3.05 (m, 4H, $H_{6,9}$), 2.91−2.69 (m, 2H, $H_{9'}$), 0.70 (t, J_{HH} = 7.1 Hz, 3H, H_{10}), 0.63 (t, J_{HH} = 7.1 Hz, 3H, $H_{10'}$). $^{13}C\{^1H\}$ NMR (75.5 MHz, $CDCl_3$): δ 166.49 (C_8), 148.27 (d, J_{CP} = 12.7 Hz, C_5), 138.82 (C_1), 131.82 ($C_{14,14'}$), 131.78 (d, J_{CP} = 100 Hz, C_{11}), 131.65 (d, J_{CP} = 9.5 Hz, C_{12}), 131.40 (d, J_{CP} = 9.5 Hz, $C_{12'}$), 130.56 (d, J_{CP} = 99.0 Hz, $C_{11'}$), 128.37 (C_3), 128.29 (d, J_{CP} = 11.2 Hz, C_{13}), 128.15 (d, J_{CP} = 11.2 Hz, $C_{13'}$), 125.60 (C_4), 124.41 (C_2), 42.33 (C_9), 40.71 ($C_{9'}$), 38.31 (d, J_{CP} = 62.6 Hz, C_7), 31.19 (C_6), 13.70 (C_{10}), 12.50 ($C_{10'}$). FTIR (KBr, cm^{-1}): 3064, 2980, 2931, 2874, 1634 ($\nu_{C=O}$), 1485, 1437, 1380, 1360, 1323, 1282, 1269, 1242 (ν_{N-O}), 1227, 1200, 1180 ($\nu_{P=O}$), 1151, 1136, 1119, 1099, 1068, 997, 970, 893, 877, 862, 835, 783, 766, 746, 714, 700, 617, 553, 532, 517, 490. HRMS (ESI) m/z (%): 423.1828 (100) [M + H^+]. $C_{24}H_{28}N_2O_3P$ requires 423.1838; 445.1637 (32) [M + Na^+]. $C_{24}H_{27}N_2O_3PNa$ requires 445.1657. Anal. Calcd for $C_{24}H_{27}N_2O_3P$: C 68.23, H 6.44, N 6.63. Found: C 67.79, H 6.65, N 6.59.

*2,6-Bis(diphenyl-N,N-diethylcarbamoylmethylphosphine oxide)-pyridine (**9**$_N$).* A solution of *n*-BuLi (1.6 M in hexane, 56.3 mL, 90.1 mmol) was added dropwise (23 °C, 30 min) under nitrogen to a vigorously stirred slurry of 2,6-bis(diphenylphosphinoylmethyl)-pyridine[31b] (20.28 g, 40 mmol) in dry toluene (250 mL). The solid dissolves, and the solution turns red during the addition. Following addition, the solution was heated (80−90 °C, 2 h), and then cooled (23 °C), and diethylcarbamyl chloride (10.1 mL, 80 mmol), in dry toluene (50 mL), was added dropwise (30 min) with vigorous stirring. The mixture was heated and stirred (90 °C, 12 h), and a yellow suspension was formed. The mixture was poured into an ice bath (100 g), and the phases separated. The aqueous layer was extracted with $CHCl_3$ (3 × 50 mL), and the combined organic phases were dried (4 Å molecular sieves) and filtered and the volatiles removed by vacuum evaporation. A light brown residue was recovered, dispersed with acetone (10 mL), filtered, washed with diethyl ether (3 × 25 mL), and vacuum-dried leaving a white solid (**9**$_N$): yield 8.7 g, 31% (*rac/meso* 80/20); mp 179−184 °C. The isomeric mixture is soluble in $CHCl_3$, CH_2Cl_2, MeOH, and EtOH, partially soluble in acetone, and insoluble in toluene, ethyl acetate, pentane, and Et_2O. $^{31}P\{^1H\}$ NMR (121.5 MHz, $CDCl_3$): δ 30.2. ^1H NMR (300 MHz, $CDCl_3$): δ 7.86 (dd, J_{HH} = 7.1 Hz, 4H, H_9), 7.72 (dd, J_{HH} = 7.1 Hz, 4H, $H_{9'}$), 7.51−7.32 (m, 15H, $H_{1,2,10,10',11,11'}$), 5.24 (d, J_{HP} = 13.8 Hz, 2H, H_4), 3.31−3.01 (m, 8H, $H_{6,6'}$), 0.92 (t, J_{HH} = 7.1 Hz, 6H, H_7), 0.86 (t, J_{HH} = 7.0 Hz, 6H, $H_{7'}$). $^{13}C\{^1H\}$ NMR (75.5 MHz, $CDCl_3$): δ 166.14 (C_5), 151.94 (d, J_{CP} = 5.6 Hz, C_3), 137.01 (C_1), 132.29 (d, J_{CP} = 9.5 Hz, C_9), 132.12 (d, J_{CP} = 101 Hz, C_8), 132.01 (d, J_{CP} = 9.0 Hz, $C_{9'}$), 131.76 (C_{11}), 131.70 ($C_{11'}$), 131.47 (d, J_{CP} = 102 Hz, $C_{8'}$), 128.14 (d, J_{CP} = 11.6 Hz, $C_{10,10'}$), 123.78 (C_2), 55.93 (d, J_{CP} = 64.7 Hz, C_4), 42.98 (C_6), 40.90 ($C_{6'}$), 14.68 (C_7), 12.71 ($C_{7'}$). FTIR (KBr, cm^{-1}): 3057, 2978, 2936, 1643 ($\nu_{C=O}$), 1439, 1200 ($\nu_{P=O}$). HRMS(ESI): m/z (%): 706.2983 (100) [M + H^+]. $C_{41}H_{46}N_3O_4P_2$ requires 706.2964; 728.2787 (11) [M + Na^+]. $C_{41}H_{45}N_3O_4P_2Na$ requires 728.2783.

*2,6-Bis(diphenyl-N,N-diethylcarbamoylmethylphosphine oxide)-pyridine N-Oxide (**9**).* Method A is described here. A sample of **9**$_N$ (7.87 g, 11.2 mmol, *rac/meso* 80/20) was dissolved in a mixture of glacial acetic acid (30 mL) and aqueous H_2O_2 solution (30%, 6.3 mL, 56 mmol) and the mixture stirred (23 °C, 4 d). The resulting solution was vacuum evaporated leaving a white solid that was dissolved in $CHCl_3$ (50 mL) and washed with distilled water (3 × 25 mL). The organic phase was dried (4 Å molecular sieves) and filtered, and the volatiles were removed by vacuum evaporation. The residue was dissolved in acetone (15 mL) and the solution treated with diethyl ether (100 mL). A precipitate formed that was collected by filtration and washed with diethyl ether (3 × 10 mL) leaving a colorless

microcrystalline powder (**9**): yield 3.96 g, 47% (*rac/meso* > 95/5). The filtrate was vacuum evaporated leaving additional **9** as a white powder: yield 2.28 g, 27% (*rac/meso* 54/46); global yield 6.24 g, 74% (*rac/meso* 80/20). Method B follows. To a solution of $\mathbf{9_N}$ (1.0 g, 1.41 mmol, *rac/meso* 80/20) in anhydrous CH_2Cl_2 (10 mL) was slowly added *m*-chloroperoxybenzoic acid (77 wt %, 635 mg, 2.83 mmol), and the mixture was stirred (23 °C, 12 h). The resulting reaction mixture was diluted in CH_2Cl_2 (50 mL) and washed with aqueous NaOH (2 N, 4 × 10 mL) and then distilled water (2 × 10 mL). The organic phase was dried (anhydr $MgSO_4$) and filtered, and the solvents were removed by vacuum evaporation, leaving **9** as a white powder: yield 1.02 g, 100% (*rac/meso* 80/20); mp *rac*-**9**: 172−174 °C. $^{31}P\{^1H\}$ NMR (121.5 MHz, $CDCl_3$) *rac*-**9**: δ 29.6. *meso*-**9**: δ 31.3. In d_4-MeOH: *rac*-**9**: δ 35.0. *meso*-**9**:δ 36.4. ^1H NMR (300 MHz, $CDCl_3$) *rac*-**9**: δ 8.03 (d, J_{HH} = 8.1 Hz, 2H, H_2), 7.82−7.74 (m, 8H, $H_{9,9'}$), 7.49−7.28 (m, 12H, $H_{10,10',11,11'}$), 7.10 (t, J_{HH} = 8.0 Hz, 1H, H_1), 6.62 (d, J_{HH} = 9.5 Hz, 2H, H_4), 3.34−2.95 (m, 8H, $H_{6,6'}$), 0.85 (t, J_{HH} = 7.2 Hz, 6H, H_7), 0.82 (t, J_{HH} = 7.2 Hz, 6H, $H_{7'}$). *meso*-**9**: 7.92−7.75 (m, 10H, $H_{2,9,9'}$), 7.49−7.27 (m, 12H, $H_{10,10',11,11'}$), 6.84 (t, J_{HH} = 8.1 Hz, 1H, H_1), 6.82 (d, J_{HH} = 12.2 Hz, 2H, H_4), 3.38−2.93 (m, 8H, $H_{6,6'}$), 0.91 (t, J_{HH} = 7.1 Hz, 6H, H_7), 0.84 (t, J_{HH} = 7.1 Hz, 6H, $H_{7'}$).$^{13}C\{^1H\}$ NMR (75.5 MHz, $CDCl_3$) *rac*-**9**: δ 164.64 (d, J_{CP} = 2.6 Hz, C_5), 142.26 (C_3), 132.07 ($C_{11,11'}$), 131.91 (d, J_{CP} = 102 Hz, C_8), 131.60 (d, J_{CP} = 9.5 Hz, C_9), 131.54 (d, J_{CP} = 9.5 Hz, $C_{9'}$), 131.02 (d, J_{CP} = 102 Hz, $C_{8'}$), 128.52−128.15 ($C_{1,10,10'}$), 124.91 (C_2), 42.79 (C_6), 42.59 (d, J_{CP} = 64.4 Hz, C_4), 41.04 ($C_{6'}$), 14.26 (C_7), 12.61 ($C_{7'}$). *meso*-**9**: δ 164.75 (d, J_{CP} = 2.5 Hz, C_5), 143.17 (C_3), 132.71−130.49 ($C_{8,8',9,9',11,11'}$), 128.96−128.21 ($C_{10,10'}$), 127.87 (C_1), 124.58 (C_2), 43.30 (d, J_{CP} = 63.6 Hz, C_4), 42.89 (C_6), 41.12 ($C_{6'}$), 14.15 (C_7), 12.69 ($C_{7'}$). FTIR (KBr, cm^{-1}): 3057, 2976, 2932, 1643 ($\nu_{C=O}$), 1556, 1483, 1429, 1400, 1313, 1275 (ν_{N-O}), 1203 ($\nu_{P=O}$), 1126, 1103, 1072, 997, 902, 841, 727, 706, 696, 534, 507. HRMS (ESI) *m/z* (%): 722.2904 (100) [M + H^+]. $C_{41}H_{46}N_3O_5P_2$ requires 722.2913. Anal. Calcd for $C_{41}H_{45}N_3O_5P_2$: C 68.23, H 6.28, N 5.82. Found: C 67.74, H 6.39, N 5.60.

*2,6-Bis[(diphenyl-N,N-diethylcarbamoylmethylphosphine oxide)-methyl]pyridine (**10**$_N$).* A solution of *n*-BuLi (1.6 M in hexane, 31.3 mL, 50 mmol) was added dropwise (23 °C, 40 min), under nitrogen, to a vigorously stirred solution of diphenyl-*N,N*-diethylcarbamoylmethylphosphine oxide[38] (15.75 g, 50 mmol) in toluene (300 mL). Following combination of the reagents, a clear, pale yellow solution was obtained that was heated (75−80 °C, 2 h) and stirred. The resulting dark red solution was cooled (23 °C) and transferred dropwise over 1 h, under nitrogen, into a vigorously stirred solution of 2,6-(dibromomethyl)pyridine[39] (6.63 g, 25 mmol) in toluene (100 mL, −40 °C). The resulting mixture was slowly warmed (23 °C), stirred, and then heated (80 °C). After about 2 h a yellow precipitate appeared, and heating and stirring were continued (12 h). The resulting mixture was cooled, the solid was collected by filtration and washed with water (100 mL), and the remaining solid dissolved in $CHCl_3$ (50 mL). The aqueous layer was extracted with $CHCl_3$ (2 × 25 mL), the combined organic phases were dried (4 Å molecular sieves) and filtered and the volatiles removed by vacuum evaporation leaving a pale yellow residue. The residue was washed with Et_2O (3 × 25 mL) leaving a white powder ($\mathbf{10_N}$) consisting of a diasteroisomeric mixture of racemic isomers (*R,R/S,S*) and mesomeric isomer (*R,S*): yield 9.0 g, 49% (*rac/meso* 60/40). The combined filtrate was vacuum evaporated, and the residue was dissolved in a minimum of EtOAc (1 mL) and diethyl ether (20 mL). The resulting precipitate was collected by filtration and washed with diethyl ether (10 mL): yield 2.2 g, 12% (*rac/meso* 13/87); global yield 11.2 g, 61% (*rac/meso* 51/49). The compound is soluble in $CHCl_3$, CH_2Cl_2, MeOH, and EtOH, slightly soluble in benzene, toluene, acetone, and EtOAc, and insoluble in pentane and Et_2O. Details for diastereoisomeric resolution follow: In a 100 mL round-bottom flask, 350 mg of $\mathbf{10_N}$ (*rac/meso* 60/40) was dissolved in CH_2Cl_2/acetone (1/1, 2 mL), and diethyl ether (60 mL) was added. The solvent was allowed to slowly evaporate (23 °C). After one day, block-like crystals of racemic (*R,R/S,S*) isomers were separated from the solution containing the *meso* isomer (*R,S*) and washed several time with diethyl ether. The same procedure was repeated a second time for each isomer: yield *rac*-$\mathbf{10_N}$ 160 mg, 46%, *meso*-$\mathbf{10_N}$ 80 mg, 23%; mp *rac*-$\mathbf{10_N}$ 186−188 °C; *meso*-$\mathbf{10_N}$ 140−142 °C. $^{31}P\{^1H\}$ NMR (121.5 MHz, $CDCl_3$) *rac*-$\mathbf{10_N}$: δ 30.4. *meso*-$\mathbf{10_N}$: δ 30.4. ^1H NMR (300 MHz, $CDCl_3$) *rac*-$\mathbf{10_N}$: δ 8.15 (t, J_{HH} = 8.7 Hz, 4H, H_{10}), 7.91 (t, J_{HH} = 8.6 Hz, 4H, $H_{10'}$), 7.45 (m, 12H, $H_{11,11',12,12'}$), 7.26 (t, J_{HH} = 7.4 Hz, 1H, H_1), 6.84 (d, J_{HH} = 7.4 Hz, 2H, H_2) 4.30 (t, J_{HP} = 13.1 Hz, 2H, H_5), 3.42−3.32 (m, 2H, H_7), 3.14−2.89 (m, 8H, $H_{4,7'}$), 2.66−2.59 (m, 2H, H_7), 0.61 (t, J_{HH} = 6.6 Hz, 6H, H_8), 0.41 (t, J_{HH} = 6.7 Hz, 6H, $H_{8'}$). *meso*-$\mathbf{10_N}$: δ 8.27 (t, J_{HH} = 8.9 Hz, 4H, H_{10}), 7.85 (t, J_{HH} = 9.1 Hz, 4H, $H_{10'}$), 7.53−7.40 (m, 12H, $H_{11,11',12,12'}$), 7.30 (t, J_{HH} = 9.4 Hz, 1H, H_1), 6.87 (d, J_{HH} = 7.6 Hz, 2H, H_2) 4.14 (t, J_{HP} = 13.1 Hz, 2H, H_5), 3.50−3.45 (m, 2H, H_7), 3.30−3.04 (m, 8H, $H_{4,7'}$), 2.91−2.82 (m, 2H, H_7), 0.80 (t, J_{HH} = 6.9 Hz, 6H, H_8), 0.69 (t, J_{HH} = 6.9 Hz, 6H, $H_{8'}$).$^{13}C\{^1H\}$ NMR (75.5 MHz, $CDCl_3$) *rac*-$\mathbf{10_N}$: δ 167.43 (C_6), 158.05 (d, J_{CP} = 15.1 Hz, C_3), 136.68 (C_1), 132.07 (d, J_{CP} = 9.5 Hz, C_{10}), 131.86 ($C_{12,12'}$), 131.79 (d, J_{CP} = 9.5 Hz, $C_{10'}$), 130.76 (C_9), 130.69 ($C_{9'}$), 128.40 (d, J_{CP} = 11.9 Hz, C_{11}), 128.34 (d, J_{CP} = 11.4 Hz, $C_{11'}$), 121.89 (C_2), 46.03 (d, J_{CP} = 62.0 Hz, C_5), 42.30 (C_7), 40.57 ($C_{7'}$), 36.39 (C_4), 13.51 (C_8), 12.30 ($C_{8'}$). *meso*-$\mathbf{10_N}$: δ 168.27 (C_6), 158.32 (d, J_{CP} = 13.8 Hz, C_3), 136.64 (C_1), 132.47 (d, J_{CP} = 9.3 Hz, C_{10}), 131.96 (d, J_{CP} = 9.3 Hz, $C_{10'}$), 131.90 (C_{12}), 131.72 (d, J_{CP} = 75.5 Hz, C_9), 131.67 ($C_{12'}$), 131.19 (d, J_{CP} = 75.5 Hz, $C_{9'}$), 128.54 (d, J_{CP} = 12.5 Hz, C_{11}), 128.38 (d, J_{CP} = 12.5 Hz, $C_{11'}$), 121.64 (C_2), 46.51 (d, J_{CP} = 61.2 Hz, C_5), 42.68 (C_7), 40.92 ($C_{7'}$), 36.50 (C_4), 13.88 (C_8), 12.69 ($C_{8'}$). FTIR (KBr, cm^{-1}): 3059, 2976, 2934,1634 ($\nu_{C=O}$), 1437, 1379, 1319, 1209, 1190 ($\nu_{P=O}$), 1113. HRMS (ESI) *m/z* (%): *rac*-$\mathbf{10_N}$ 734.3268 (94) [M + H^+]. $C_{43}H_{50}N_3O_4P_2$ requires 734.3277; 756.3094 (100) [M + Na^+]. $C_{43}H_{49}N_3O_4P_2Na$ requires 756.3096; *meso*-$\mathbf{10_N}$ 734.3264 (53) [M + H^+]. $C_{43}H_{50}N_3O_4P_2$ requires 734.3277; 756.3091 (100) [M + Na^+]. $C_{43}H_{49}N_3O_4P_2Na$ requires 756.3096.

*2,6-Bis[(diphenyl-N,N-diethylcarbamoylmethylphosphine oxide)-methyl]pyridine N-Oxide (**10**).* Method A is described here. To a solution of $\mathbf{10_N}$ (7.42 g, 10 mmol, *rac/meso* 60/40) in glacial acetic acid (30 mL) was added a hydrogen peroxide (30%, 6 mL, 53 mmol). The mixture was stirred (23 °C, 4 d), and the volatiles were removed by vacuum evaporation. The residue was dissolved in $CHCl_3$ (100 mL) and washed with distilled water (3 × 25 mL). The organic phase was dried (4 Å molecular sieves) and filtered, and the volatiles were removed by vacuum evaporation leaving **10** as white powder: yield 5.56 g, 74% (*rac/meso* 60/40). Method B follows. To a solution of $\mathbf{10_N}$ (1.0 g, 1.36 mmol, *rac/meso* 60/40) in anhydrous CH_2Cl_2 (10 mL) was slowly added *m*-chloroperoxybenzoic acid (77 wt %, 613 mg, 2.72 mmol). The mixture was stirred (23 °C, 12 h), and the resulting mixture was diluted with CH_2Cl_2 (50 mL) and washed with aqueous NaOH (2 N, 3 × 15 mL) and distilled water (2 × 10 mL). The organic phase was dried (anhydr $MgSO_4$) and filtered, and the volatiles were removed by vacuum evaporation leaving **10** as a white powder: yield 990 mg, 97% (*rac/meso* 60/40). Diastereomerically pure isomers of **10** were also prepared starting with diastereomerically pure isomers of $\mathbf{10_N}$; mp *rac*-**10** 128−130 °C; *meso*-**10** 108−110 °C. The compound is soluble in $CHCl_3$, CH_2Cl_2, MeOH, and EtOH, slightly soluble in xylenes, toluene, benzene, acetone, ethyl acetate, and THF, and insoluble in Et_2O and heptane. $^{31}P\{^1H\}$ NMR (121.5 MHz, $CDCl_3$) *rac*-**10**: δ 32.5. *meso*-**10**: δ 30.8. In d_4-MeOH *rac*-**10**: δ 35.1. *meso*-**10**: δ 33.7. ^1H NMR (300 MHz, $CDCl_3$) *rac*-**10**: δ 8.12−8.06 (m, 4H, H_{10}), 7.95−7.89 (m, 4H, $H_{10'}$), 7.52−7.49 (m, 12H, $H_{11,11',12,12'}$), 7.07 (d, J_{HH} = 7.6 Hz, 2H, H_2), 6.89 (t, J_{HH} = 7.6 Hz, 1H, H_1), 4.92 (m, 2H, H_5), 3.52−3.44 (m, 2H, H_7), 3.30−2.92 (m, 8H, $H_{4,7'}$), 2.79−2.72 (m, 2H, H_7), 0.71 (t, J_{HH} = 6.9 Hz, 6H, H_8), 0.67 (t, J_{HH} = 7.0 Hz, 6H, $H_{8'}$). *meso*-**10**: δ 7.99−7.93 (m, 4H, H_{10}), 7.83−7.77 (m, 4H, $H_{10'}$), 7.51−7.35 (m, 12H, $H_{11,11',12,12'}$), 6.96 (d, J_{HH} = 7.6 Hz, 2H, H_2), 6.73 (t, J_{HH} = 7.7 Hz, 1H, H_1), 4.83 (q, J_{HP} = 8.1 Hz, 2H, H_5), 3.56−3.46 (m, 2H, H_7), 3.32−3.16 (m, 6H, $H_{4,7'}$), 2.99−2.89 (m, 4H, $H_{7,7'}$), 0.94 (t, J_{HH} = 7.0 Hz, 6H, H_8), 0.75 (t, J_{HH} = 7.1 Hz, 6H, $H_{8'}$). $^{13}C\{^1H\}$ NMR (75.5 MHz, $CDCl_3$) *rac*-**10**: δ 168.89 (C_6), 148.28 (d, J_{CP} = 13.2 Hz, C_3), 132.10 (d, J_{CP} = 9.5 Hz, $C_{10,10'}$), 132.04 ($C_{12,12'}$), 131.84 (d, J_{CP} = 100.2 Hz, C_9), 131.13 (d, J_{CP} = 99.7 Hz, $C_{9'}$), 128.52 (d+d, J_{CP} = 12.3 Hz, $C_{11,11'}$), 126.83 (C_2), 124.77 (C_1), 42.60 (C_7), 41.08 ($C_{7'}$), 39.33 (d, J_{CP} = 62.0 Hz, C_5), 31.72 (C_4), 13.74 (C_8), 12.74 ($C_{8'}$). *meso*-**10**: δ 167.28 (C_6), 147.63 (d, J_{CP} = 9.3 Hz, C_3), 132.03 (d, J_{CP} = 99.0 Hz, C_9), 131.94 ($C_{12,12'}$), 131.70 (d, J_{CP} = 9.1 Hz, C_{10}), 131.36 (d, J_{CP} =

9.1 Hz, $C_{10'}$), 131.29 (d, J_{CP} = 99.0 Hz, $C_{9'}$), 128.31 (d, J_{CP} = 12.2 Hz, C_{11}), 128.10 (d, J_{CP} = 11.9 Hz, $C_{11'}$), 126.72 (C_2), 124.16 (C_1), 42.53 (C_7), 40.81 ($C_{7'}$), 38.89 (d, J_{CP} = 63.3 Hz, C_5), 31.44 (C_4), 13.99 (C_8), 12.58 ($C_{8'}$). FTIR (KBr, cm^{-1}): 3057, 2974, 2934, 1632 ($\nu_{C=O}$), 1487, 1458, 1435, 1381, 1317, 1253 (ν_{N-O}), 1186 ($\nu_{P=O}$), 1117, 1097, 1072, 997, 885, 858, 833, 787, 744, 702, 555, 513. HRMS (ESI) m/z (%): 750.3228 (60) [M + H^+]. $C_{43}H_{50}N_3O_5P_2$ requires 750.3226; 772.3062 (100) [M + Na^+]. $C_{43}H_{49}N_3O_5P_2Na$ requires 772.3045. Anal. Calcd for $C_{43}H_{49}N_3O_5P_2$: C 68.88, H 6.59, N 5.60. Found: C 66.21, H 6.73, N 5.19.

Lanthanide Complex Syntheses. The lanthanide coordination complexes were prepared by combination of 1 equiv of ligand with 1 equiv of $Ln(NO_3)_3{\cdot}xH_2O$ in MeOH. The mixtures were stirred (23 °C, 2 h), volatiles removed by vacuum evaporation, and the resulting powders vacuum-dried. Elemental analyses (CHN) and infrared spectra for representative samples were obtained, and selected samples were crystallized in order to obtain single crystals for X-ray diffraction analyses. Characterization data for the Pr(III) complexes are summarized here, and additional data are provided in Supporting Information. [Pr(**7**)$(NO_3)_3$]·$4H_2O$. FTIR (KBr, cm^{-1}): 1601 (ν_{CO}), 1211 (ν_{NO}), 1134 (ν_{PO}). Anal. Calcd for $C_{23}H_{33}N_5O_{16}PPr$: C, 34.21; H, 4.12; N, 8.67. Found: C, 34.62; H, 3.85; N, 8.44. [Pr(**8**)-$(NO_3)_3$]·MeOH. FTIR (KBr, cm^{-1}): 1601 (ν_{CO}), 1227 (ν_{NO}), 1151 (ν_{PO}). Anal. Calcd for $C_{25}H_{31}N_5O_{13}PPr$: C, 38.43; H, 4.00; N, 8.96. Found: C, 38.07; H 3.97; N, 8.97. [Pr(**9**)$(NO_3)_3$]·$4H_2O$. FTIR (KBr, cm^{-1}): 1637 (ν_{CO}), 1612 (ν_{CO}), 1246 (ν_{NO}), 1148 (ν_{PO}). Anal. Calcd for $C_{41}H_{53}N_6O_{18}P_2Pr$: C, 43.91; H, 4.77; N, 7.50. Found: C, 43.77; H, 4.38; N, 7.22. {[Pr(**10**)$(NO_3)(H_2O)]_2$(μ-**10**)}$(NO_3)_4$·$12H_2O$. FTIR (KBr, cm^{-1}): 1620 (ν_{CO}), 1597 (ν_{CO}), 1213 (ν_{NO}), 1153 (ν_{PO}). Anal. Calcd for $C_{129}H_{175}N_{15}O_{47}P_6Pr_2$: C, 49.10; H, 5.59; N, 6.66. Found: C, 49.24; H, 5.62; N, 6.62.

Photophysical Characterization. Solutions for spectroscopic studies were prepared in a glovebox with controlled nitrogen atmosphere (O_2 < 0.5 ppm, H_2O < 1 ppm). A sample of [Eu(**9**)$(NO_3)_3$] (17 mg) was initially dissolved in methanol (3 mL) and stirred (15 min). After measurement in methanol, the solvent was evaporated, and the sample was redissolved in deuterated methanol (5 mL) for the spectroscopic measurements. Solutions were equilibrated for at least two days before measurements were made. The emission spectrum and lifetimes were measured on a Jobin-Yvon Fluorolog-3 spectrofluorimeter equipped with a red-sensitive PMT R928 detector and a Xe flash lamp. The excitation wavelength was 289 nm, and emission and excitation slits were 5 nm for the spectra and 9 nm for the lifetime measurements. Additionally, for the lifetime measurements, a time-per-flash of 41 ms, a flash count of 100, an initial delay of 0.06 ms, a sample width and maximum delay of 4 ms for methanol and 6 ms for deuterated methanol, and a delay interval of 0.01 ms were chosen. The number of coordinated methanol molecules q was determined through comparison of the emission lifetimes of Eu(III) in methanol and deuterated methanol, using the equation $q = 2.1(\tau^{-1}_{MeOH} - \tau^{-1}_{MeOD})$ proposed by Horrocks and Sudnick.[40] All reported lifetimes are the average of at least three independent measurements. Emission spectroscopy for a microcrystalline sample of the complex was examined by using a home-built scanning conformal microscope spectrometer. Briefly, laser excitation from either an argon-ion or a krypton-ion source was focused to a diffraction-limited spot, and the signal was collected in a backscattering geometry. Scattered excitation was removed by using long-pass edge filters, and the PL spectrum was dispersed and read-out using a CCD spectrograph. Spectra were not corrected for instrument response.

X-ray Diffraction Analyses. Crystals of the ligands and lanthanide complexes were coated with Paratone oil and mounted on a CryoLoop attached to a metal pin with epoxy. Diffraction data were collected with a Bruker X8 Apex II CCD-based X-ray diffractometer equipped with an Oxford Cryostream 700 low temperature device and normal focus Mo-target X-ray tube (λ = 0.710 73 Å) operated at 1500 W power (50 kV, 30 mA). Data collection and processing were accomplished with the Bruker APEX2 software suite.[41] The structures were solved by direct methods and refined with full-matrix least-squares methods on F^2 with use of SHELXTL.[42] Lattice and data collection parameters for the ligands and the metal complexes are presented in Tables 1 and 2, respectively. All heavy atoms were refined anisotropically, and hydrogen atoms were included in ideal positions and refined isotropically (riding model) with $U_{iso} = 1.2U_{eq}$ of the parent atom ($U_{iso} = 1.5U_{eq}$ for methyl groups) unless noted otherwise. The structure refinements were well behaved except as indicated in the following notes. $(7)_2{\cdot}CH_2Cl_2$: colorless rods were obtained by slow evaporation of a CH_2Cl_2/hexane (2/1) solution. Lattice CH_2Cl_2 chlorine atoms are disordered over two sites with occupancies set at 65/35. **8**: colorless prisms were obtained by slow evaporation of an acetone/EtOAc (4/1) solution. **9**: colorless platelets were obtained by slow evaporation of an Et_2O solution containing small amounts of acetone and CH_2Cl_2. [Pr(7_R)$(NO_3)_3(Me_2CO)$]: green rods grown from slow evaporation of an acetone/EtOAc (1/1) solution of the complex formed from a 1:1 combination of 7 (*rac*) and Pr-$(NO_3)_3{\cdot}6H_2O$ in MeOH. [Pr(8_R)$(NO_3)_3$(MeOH)-Pr(8_S)-$(NO_3)_3$(MeOH)]$_n$: green rods formed from slow evaporation of MeOH solution of the complex formed from a 1:1 combination of **8** (*rac*) and $Pr(NO_3)_3{\cdot}6H_2O$. The O−H hydrogen atoms on the inner sphere methanol molecules were located in the difference map. All atoms of one nitrate group, N10, O22, O23, O24, and one O-atom, O19, of a second nitrate are disordered over two sites with occupancies set at 60/40. Disordered lattice solvent molecules, likely either H_2O or MeOH or a combination, were not adequately modeled. Refinement was improved by application of the SQUEEZE procedure.[43] PLATON estimates 64 electrons unaccounted for in the solvent accessible void volume of 135 $Å^3$. {[Eu($9_{R,S}$)-$(NO_3)_3$]·$(Me_2CO)_{0.75}{\cdot}(H_2O)_{0.3}$}$_4$: colorless blocks were formed by slow evaporation of a acetone/MeOH (4/1) solution of the complex obtained from a 1:1 combination of **9** (*rac*/*meso* 54/46) and

Table 1. Crystallographic Data for Ligands $(7)_2{\cdot}CH_2Cl_2$, 8_R, and $9_{R,R}$

	$(7)_2{\cdot}CH_2Cl_2$	8_R	$9_{R,R}$
empirical formula	$C_{47}H_{52}Cl_2N_4O_6P_2$	$C_{24}H_{27}N_2O_3P$	$C_{41}H_{45}N_3O_5P_2$
crystal size (mm^3)	0.12 × 0.17 × 0.51	0.37 × 0.53 × 0.57	0.19 × 0.23 × 0.56
fw	901.77	422.45	721.74
cryst syst	triclinic	triclinic	orthorhombic
space group	*P*1	*P*1	*Aba*2
unit cell dimens			
a (Å)	11.9000(8)	10.6641(5)	22.2182(16)
b (Å)	19.5305(13)	14.2715(6)	15.4755(12)
c (Å)	20.4598(13)	16.8816(9)	10.8569(9)
α (deg)	101.122(4)	106.043(3)	90
β (deg)	90.588(4)	99.900(4)	90
γ (deg)	99.922(4)	109.529(4)	90
V ($Å^3$)	4591.4(5)	2225.9(2)	3733.0(5)
Z	4	4	4
T (K)	173(2)	173(2)	173(2)
D_{calcd} (g cm^{-3})	1.305	1.261	1.284
μ (mm^{-1})	0.263	0.151	0.165
min/max transm	0.8765/0.9691	0.9184/0.9462	0.9131/0.9696
reflns collected	43 055	25 550	21 088
indep reflns [R_{int}]	18 761 [0.0743]	9792 [0.0656]	4645 [0.0917]
final R indices [$I > 2\sigma(I)$] R1 (wR2)	0.0705 (0.1612)	0.0538 (0.1119)	0.0515 (0.0980)
final R indices (all data) R1 (wR2)	0.1419 (0.1935)	0.1053 (0.1335)	0.0980 (0.1124)

Table 2. Crystallographic Data for Coordination Complexes

	$[Pr(\mathbf{7}_R)(NO_3)_3(Me_2CO)]$	$[Pr(\mathbf{8}_R)(NO_3)_3(MeOH)Pr(\mathbf{8}_S)(NO_3)_3(MeOH)]$	$\{[Eu(\mathbf{9}_{R,S})(NO_3)_3]\cdot(Me_2CO)_{0.75}\cdot(H_2O)_{0.3}\}_4$	$[Pr(\mathbf{9}_{R,S})(NO_3)_3]$	$[Er(\mathbf{9}_{R,S})(NO_3)_3]\cdot Me_2CO$	$[Er(\mathbf{9}_{S,S})(NO_3)_2(H_2O)](NO_3)\cdot(MeOH)(H_2O)_{0.4}$	$\{[Pr(\mathbf{10}_{R,S})(NO_3)(H_2O)]_2(\mu\text{-}\mathbf{10}_{R,R})\}(NO_3)_4$
empirical formula	$C_{26}H_{31}N_5O_{13}PPr$	$C_{50}H_{62}N_{10}O_{26}P_2Pr_2$	$C_{173}H_{201.4}Eu_4N_{24}O_{60.2}P_8$	$C_{41}H_{45}N_6O_{14}P_2Pr$	$C_{44}H_{51}ErN_6O_{15}P_2$	$C_{42}H_{51.8}ErN_6O_{16.4}P_2$	$C_{129}H_{151}N_{13}O_{29}P_6Pr_2$
cryst size (mm^3)	0.12 × 0.24 × 0.48	0.09 × 0.13 × 0.30	0.24 × 0.32 × 0.52	0.22 × 0.20 × 0.18	0.26 × 0.36 × 0.67	0.23 × 0.24 × 0.26	0.23 × 0.35 × 0.86
fw	793.44	1562.86	4435.78	1048.68	1133.11	1132.29	2691.25
cryst syst	monoclinic	triclinic	orthorhombic	orthorhombic	monoclinic	monoclinic	monoclinic
space group	$P2_1/c$	$P1$	$Pbca$	$Pbca$	$P2_1/c$	$P2_1/c$	$C2/c$
unit cell dimens							
a (Å)	19.648(1)	10.933(3)	18.5482(7)	22.512(1)	14.1511(4)	9.7694(8)	31.687(4)
b (Å)	9.3662(6)	17.548(5)	22.617(1)	18.6045(8)	20.7534(5)	22.468(2)	26.926(3)
c (Å)	19.485(1)	18.038(5)	22.8902(8)	22.768(1)	17.7301(4)	22.266(2)	17.310(2)
α (deg)	90	99.746(9)	90	90	90	90	90
β (deg)	115.749(4)	105.245(8)	90	90	111.823(1)	93.186(4)	105.915(2)
γ (deg)	90	91.715(7)	90	90	90	90	90
V ($Å^3$)	3229.9(3)	3280.6(16)	9602.7(7)	9535.8(7)	4833.9(2)	4879.8(7)	14203(3)
Z	4	2	2	8	4	4	4
T, K	173(2)	173(2)	173(2)	173(2)	173(2)	173(2)	123(2)
D_{calcd} (g cm^{-3})	1.632	1.582	1.534	1.461	1.557	1.541	1.317
μ (mm^{-1})	1.628	1.602	1.446	1.157	1.875	1.860	0.818
min/max transm	0.5105/0.8323	0.6450/0.8706	0.5225/0.7202	0.7808/0.8153	0.365/0.641	0.6395/0.6722	0.5385/0.8317
reflns collected	28 262	23 665	15 387	189 747	64 148	67 853	52 198
indep reflns [R_{int}]	7096[0.1604]	12 870 [0.0843]	15 400	10 934 [0.0656]	11 090 [0.0688]	12 089 [0.0576]	14 454 [0.0792]
final R indices [$I > 2\sigma(I)$] R1 (wR2)	0.1022 (0.2020)	0.0734 (0.1585)	0.0619 (0.1360)	0.0367 (0.0956)	0.0325 (0.0653)	0.0305 (0.0583)	0.0656 (0.1765)
final R indices (all data) R1 (wR2)	0.1662 (0.2266)	0.1508 (0.1844)	0.1149 (0.1625)	0.0546 (0.1017)	0.0497 (0.0716)	0.0495 (0.0647)	0.1050 (0.1965)

dx.doi.org/10.1021/ic3025342 | Inorg. Chem. 2013, 52, 3063−3083

Scheme 1

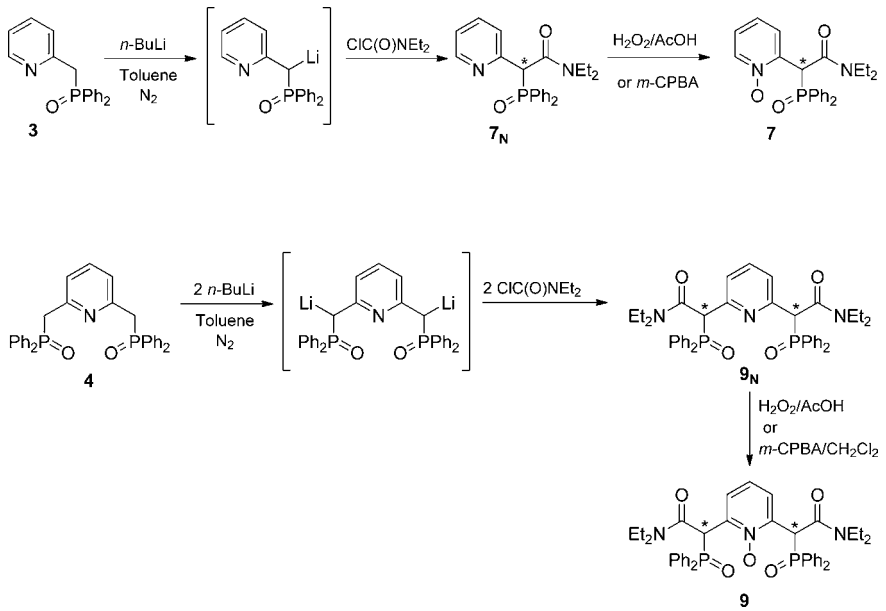

$Eu(NO_3)_3{\cdot}6H_2O$ in MeOH. The crystals were found to be twinned (three components). The non-hydrogen atoms were refined anisotropically. The H-atoms on the water (H16b, H16c) were located in the difference map and allowed to refine with constraints on the O−H bond length and H−O−H bond angle. The C27 atom was disordered over two positions that were allowed to refine freely to 75/25% occupancies with the thermal parameters constrained to be similar. Two partially occupied solvent molecules were found in the outer sphere. The acetone was set to 75% occupancy, and the water (O16) was set to 30% occupancy. $[Pr(\mathbf{9}_{R,S})(NO_3)_3]$: green platelets were obtained from slow evaporation of an acetone/MeOH solution (4/1) of the complex formed by the 1:1 combination of **9** (*rac/meso* 54/46) and $Pr(NO_3)_3{\cdot}6H_2O$ in MeOH. The lattice solvent molecules were disordered, and the SQUEEZE procedure was applied. PLATON estimates 368 electrons unaccounted for in the solvent accessible void volume of 1024 Å^3. $[Er(\mathbf{9}_{R,S})(NO_3)_3]{\cdot}Me_2CO$: pink diamond shaped crystals were deposited from the slow evaporation of a acetone/EtOAc (4/1) solution of the complex obtained from a 1:1 combination **9** (*rac/meso* 54/46) and $Er(NO_3)_3{\cdot}5H_2O$ in MeOH. $[Er(\mathbf{9}_{S,S})(NO_3)_2(H_2O)](NO_3){\cdot}(MeOH){\cdot}(H_2O)_{0.4}$: pink blocks formed in the same synthesis and crystallization described above for $[Er(\mathbf{9}_{R,S})(NO_3)_3]{\cdot}Me_2CO$. The lattice contains a methanol molecule with full occupancy and a partial water molecule that, when refined, converged with an occupancy of 40%. $\{[Pr(\mathbf{10}_{R,S})(NO_3)(H_2O)]_2(\mu\text{-}\mathbf{10}_{R,R})\}(NO_3)_4$: green rods were obtained by slow evaporation of an acetone/MeOH (4/1) solution of the complex formed from a 1:1 combination of **10** (*rac/meso* 60/40) and $Pr(NO_3)_3{\cdot}6H_2O$ in MeOH. One ethyl carbon atom, C51, is disordered, and it was modeled over two sites with 80/20 occupancies. In addition, unbound outer sphere nitrate ions and lattice solvent molecules are disordered. These were accounted for by using PLATON/SQUEEZE which found void spaces of 1120 Å^3 with an electron count of 478.

Distribution Studies. *Materials.* All salts and solvents were reagent grade and were used as received. Extraction experiments were carried out using 1,2-dichloroethane (OmniSolv, EM Science) as the diluent. The aqueous phases were prepared using nitric acid (J. T. Baker, Ultrex II) and europium nitrate (Aldrich, 99.9%). Distilled, deionized water was obtained from a Barnstead Nanopure filter system (resistivity at least 18.2 MΩ-cm) and used to prepare all the aqueous solutions. The radioisotope ^{241}Am was provided by the Radiochemical and Engineering Research Center (REDC) of ORNL. The radiotracer $^{152/154}$Eu was obtained from Isotope Products, Burbank, CA. Both were added as spikes to the aqueous phases in the sample equilibration vials in the extraction experiments.

Methods. Phases at a 1:1 organic to aqueous (O:A) phase ratio were added to 2 mL polypropylene microtubes, which were then capped and mounted by clips on a disk that was rotated in a constant-temperature air box at 25.0 ± 0.5 °C for 1 h. After the contacting period, the tubes were centrifuged for 5 min at 3000 rpm and 25 °C in a Beckman Coulter Allegra 6R temperature-controlled centrifuge. A 250 μL aliquot of each phase was subsampled and counted using a Canberra Analyst pure Ge Gamma counter. Counting times were sufficient to ensure that counting error was a small fraction of the precision of the obtained distribution ratios, considered from a combination of volumetric, replicate, and counting errors to be ±5%. Americium and europium distribution ratios were calculated as the ratio of the volumetric count rates of the ^{241}Am and $^{152/154}$Eu isotopes in each phase at equilibrium.

Molecular Mechanics Calculations. The method is described here. Geometry optimizations of the free and metal-bound forms of **7**, **8**, **9**, and **10** were carried out with the MM3 force field[44] using a points-on-a-sphere metal ion[45] as implemented in PCModel software.[46] Conformational searches to locate the most stable form for each structure were performed using the GMMX algorithm provided with this software. Input files required to repeat these calculations including additional parameters for treating the metal-dependent interactions are available as Supporting Information.

■ RESULTS AND DISCUSSION

Ligand Syntheses and Characterization. The intermediate pyridine-based platforms 2-(diphenyl-*N*,*N*-diethylcarbamoylmethylphosphine oxide)pyridine, $\mathbf{7}_N$, and 2,6-bis-(diphenyl-*N*,*N*-diethylcarbamoylmethylphosphine oxide)-pyridine, $\mathbf{9}_N$, were prepared by combination of diethylcarbamoyl chloride with the putative lithio reagents formed from the respective 2-(diphenylphosphinoylmethyl)-pyridine *P*-oxide, (DPhNPO), **3**, or 2,6-bis-(diphenylphosphinoylmethyl)pyridine *P*,*P*′ dioxide (TPhNPO-P′O′), **4**, and *n*-BuLi as summarized in Scheme 1. Compound $\mathbf{7}_N$ was isolated as a white powder containing a racemic mixture of enantiomers with an unoptimized yield of 51%, and $\mathbf{9}_N$ was obtained in 31% yield as a white, solid diastereomeric mixture of isomers *R,R/S,S* (*rac*) and *R,S* (*meso*). Both compounds are spectroscopically pure, and the compositions are supported by HRMS analyses that show high intensity $[M + H^+]$ and $[M + Na^+]$ ions. The infrared spectra display strong absorptions that

are tentatively assigned to ν_{CO} and ν_{PO} stretching modes based upon prior assignments:[31a,b,h,38] 7_N, 1634 and 1190 cm^{-1}; 9_N, 1643 and 1200 cm^{-1}, respectively. The ^{31}P NMR spectra for the compounds show a single resonance: 7_N, δ 29.5; 9_N, δ 30.2. These chemical shifts are similar to shifts reported for the component molecules $Ph_2P(O)CH_2C_5H_4N$,[31a] δ 30.2, and $Ph_2P(O)CH_2C(O)NEt_2$,[38] δ 27.9. The ^{1}H and ^{13}C NMR spectra have been fully assigned, and the shifts for the methine proton and carbon centers are noteworthy: 7_N, H_6, δ 5.31, J_{HP} = 13.2 Hz, C_6, δ 56.28, J_{CP} = 64.5 Hz; 9_N, H_4, δ 5.24, J_{HP} = 13.8 Hz, C_4, δ 55.93, J_{CP} = 64.7 Hz.[36] As expected, the coupling constants are closely comparable, but the chemical shifts are noticeably downfield from the corresponding methylene proton and carbon resonances in the component molecules: $Ph_2P(O)CH_2C_5H_4N$,[31a] δ_H 3.88, J_{HP} = 14.2, δ_{CH2} 40.7, J_{CP} = 64 Hz; $Ph_2P(O)CH_2C(O)NEt_2$,[38] δ_H 3.3, J_{HP} = 15.7 Hz, δ_{CH2} 39.4, J_{CP} = 60.9 Hz.

Subsequent N-oxidations of 7_N and 9_N were accomplished with peracetic acid or *m*-CPBA, and the target ligands, 2-(diphenyl-*N*,*N*-diethylcarbamoylmethylphosphine oxide)-pyridine *N*-oxide, **7**, and 2,6-bis[(diphenyl-*N*,*N*-diethylcarbamoylmethylphosphine oxide)]pyridine *N*-oxide, **9**, were isolated as white powders with yields of 72% and 100%, respectively. Compound **7** was obtained as a racemic mixture of enantiomers while **9** was isolated as a 80/20 *rac*/*meso* mixture. The major diastereomer was isolated by precipitation from acetone or by recrystallization from Et_2O containing a small fraction of acetone or CH_2Cl_2. The minor diastereomer was not obtained in pure form. The compound compositions were supported by CHN elemental analyses and HRMS spectra that display intense [M + H$^+$] and [M + Na$^+$] ions. The infrared spectra show strong absorptions that are tentatively assigned to ν_{CO}, ν_{NO}, and ν_{PO} on the basis of previous assignments:[31a,b,h,38] **7** 1638, 1265, 1192 cm^{-1}; **9** 1643, 1275, 1203 cm^{-1}. The ^{31}P NMR spectrum for **7** is consistent with the formation of a racemic mixture of enantiomers with a single resonance: ^{31}P δ 30.4. The ^{31}P NMR spectrum for **9**, on the other hand, shows two resonances: ^{31}P δ 29.6 (*rac*) and 31.3 (*meso*) with relative intensities 4:1. The ^{1}H and ^{13}C resonances assigned to the methine proton and carbon atoms in **7** and **9** appear at H_6 δ 6.67, J_{HP} = 8.6 Hz, C_6 δ 41.38, J_{CP} = 63.8 Hz, and H_4 δ 6.62, J_{HP} = 9.5 Hz (*rac*), δ 6.82, J_{HP} = 12.2 Hz (*meso*), C_4 δ 42.59, J_{CP} = 64.4 Hz (*rac*), δ 43.30, J_{CP} = 63.6 Hz (*meso*), respectively. The assignments for the resonances of **9** are made possible by determination of the absolute configuration of the *R*,*R* and *S*,*S* diastereomers by X-ray crystallography, *vide infra*.

The proposed molecular structures of 7_R, 7_S, and $9_{R,R}$ were confirmed by single crystal X-ray diffraction analyses.[47] Views of the molecules are shown in parts a and b in Figure 1 and in Figure 2, respectively, and selected bond lengths are summarized in Table 3. The unit cell for **7** contains four independent molecules, three of which have the *R* conformation while one has the *S* conformation. There are also two CH_2Cl_2 solvent molecules in the unit cell, one of which has a disordered Cl atom. The pyridine *N*-oxide ring in each molecule is planar, and the CMPO fragment is bonded through the central methine carbon atom at the 2-position of the pyridine ring. The P═O and C═O bond vectors are rotated out of the pyridine ring plane (P═O, 58.5−73.7°; C═O, 49.8−56.7°), and they are oriented *syn* to each other. The P═O bond lengths in the four molecules are identical, P═O$_{avg}$ = 1.485 ± 0.002 Å, and they compare favorably with the P═O bond length in the NOPO derivative $\{[2\text{-}(CF_3)C_6H_4]_2P(O)\text{-}CH_2\}C_5H_4NO$, 1.4822(9) Å,[31n] and in the CMPO molecule $Ph_2P(O)CH_2C(O)NEt_2$, 1.490(3) Å.[48] The average N−O bond length, 1.307 ± 0.005 Å, is identical to the value in $\{[2\text{-}(CF_3)C_6H_4]_2P(O)CH_2\}C_5H_4NO$, 1.306(1) Å,[31n] and the average carbonyl C═O bond length, 1.229 ± 0.011 Å, is the same as reported for the amide carbonyl bond length in $Ph_2P(O)CH_2C(O)NEt_2$, 1.226(5) Å.[48] The structure for $9_{R,R}$ contains a planar pyridine *N*-oxide ring with two CMPO fragments bonded through the methine carbon atoms at the 2- and 6- positions of the pyridine *N*-oxide ring. As in **7**, the P═O and C═O bonds in each CMPO fragment are mutually *syn* to each other. The P═O and C═O bond lengths, 1.481(2) and 1.218(4) Å, are identical to the average bond lengths in **7**, but the N−O bond length is slightly longer, 1.328(4) Å. The P═O

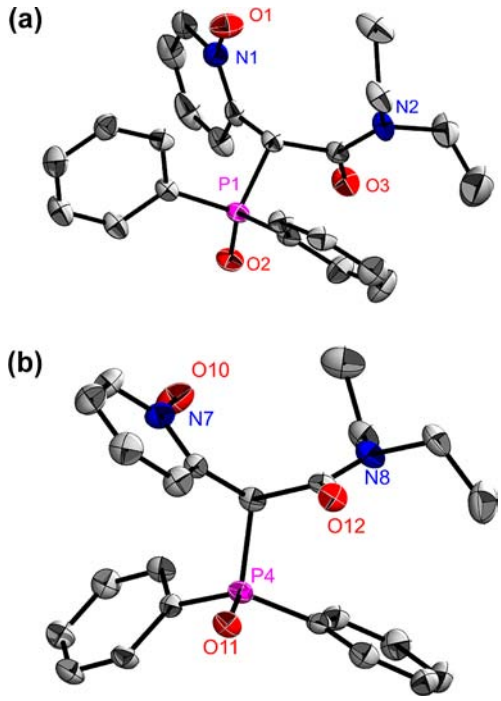

Figure 1. Molecular structure of $\{[Ph_2P(O)][C(O)NEt_2]C(H)\text{-}C_5H_4NO\}_2\cdot CH_2Cl_2$, $(7)_2\cdot CH_2Cl_2$: (a) 7_R and (b) 7_S (thermal ellipsoids, 50%) with carbon atom labels, H-atoms, and lattice CH_2Cl_2 omitted for clarity.

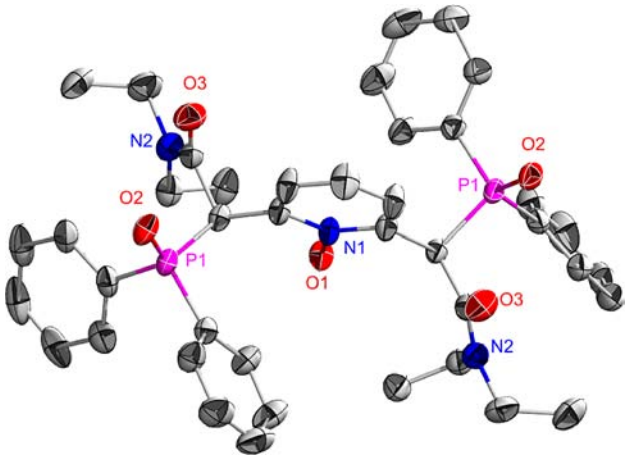

Figure 2. Molecular structure of (*R*,*R*)-$\{[Ph_2P(O)][C(O)NEt_2]C(H)\}_2C_5H_3NO$, $9_{R,R}$ (thermal ellipsoids, 50%), with carbon atom labels and H-atoms omitted for clarity.

Table 3. Selected Bond Lengths for Ligands $(7)_2{\cdot}CH_2Cl_2$, 8_R, and $9_{R,R}$ (Å)

$(7)_2{\cdot}CH_2Cl_2$	8_R	$9_{R,R}$
P−O Bond		
P1−O2 1.483(3)	P1−O3 1.4886(16)	P1−O2 1.481(2)
P2−O5 1.486(3)	P2−O6 1.4810(17)	
P3−O8 1.485(3)		
P4−O11 1.487(3)		
N−O Bond		
N1−O1 1.307(4)	N1- O1 1.311(3)	N1−O1 1.328(4)
N3−O4 1.312(4)	N3−O4 1.317(2)	
N5−O7 1.306(4)		
N7−O10 1.304(4)		
C−O Bond		
C7−O3 1.224(4)	C8−O2 1.233(3)	C5−O3 1.218(4)
C30−O6 1.231(5)	C32−O5 1.231(3)	
C53−O9 1.222(4)		
C76−O12 1.240(4)		

and N−O bond lengths are comparable with those in 2,6-$[Ph_2P(O)CH_2]_2C_5H_3NO$, 1.480(3) and 1.315(6) Å,[31b] respectively.

In order to explore potential chelate ring strain features in lanthanide ion coordination interactions of **7** and **9**, syntheses for **8** and **10** were also developed. That chemistry is summarized in Scheme 2. The respective pyridine precursors, 2-[(diphenyl-*N*,*N*-diethylcarbamoylmethylphosphine oxide)-methyl]pyridine, $\mathbf{8_N}$, and 2,6-bis[(diphenyl-*N*,*N*-diethylcarbamoylmethylphosphine oxide)methyl] pyridine, $\mathbf{10_N}$, were prepared by reaction of 2-chloromethylpyridine or 2,6-bis-(bromomethyl)pyridine with $Li\{[Ph_2P(O)][C(O)NEt_2]CH\}$, formed by combination of **1** (R = R′ = Ph, R″ = Et) and *n*-BuLi. Compound $\mathbf{8_N}$ was isolated in 50% yield as a solid, white, spectroscopically pure, racemic mixture of enantiomers. No differences between the *R* and *S* enantiomers were revealed by NMR or FTIR spectroscopy or TLC on silica plates. The proposed composition is supported by HRMS analysis that displays high intensity $[M + H^+]$ and $[M + Na^+]$ ions. The FTIR spectrum shows absorptions at 1634 and 1192 cm^{-1} that are tentatively assigned to ν_{CO} and ν_{PO} absorptions, respectively, and the ^{31}P NMR spectrum contains a single resonance at 31.0 ppm. These data are essentially identical to the data recorded for $\mathbf{7_N}$. However, distinguishing features are provided by the ^1H and ^{13}C NMR spectra. In particular, in the ^1H NMR spectrum, the CMPO fragment methine proton in $\mathbf{8_N}$ (H_7) is shifted upfield, δ 4.35, J_{HP} =12.6 Hz, relative to the value in $\mathbf{7_N}$ (H_6). Similarly, the ^{13}C NMR resonance for C_7 in $\mathbf{8_N}$ appears at δ 45.58, J_{CP} = 61.7 Hz, significantly upfield of the resonance for C_6 in $\mathbf{7_N}$.

Compound $\mathbf{10_N}$ was isolated in overall 61% yield as a diastereomeric mixture of *rac* (*R*,*R* and *S*,*S*) and *meso* (*R*,*S*) isomers with a 60/40 *rac*/*meso* ratio. The HRMS shows high intensity $[M + H^+]$ and $[M + Na^+]$ ions, and the FTIR spectrum displays absorptions at 1634 and 1190 cm^{-1} tentatively assigned to ν_{CO} and ν_{PO}, respectively. On a small scale, separation of the *rac* and *meso* forms was accomplished by recrystallization from Et_2O containing small fractions of CH_2Cl_2 or acetone. One diastereomeric pair, subsequently identified as the racemic *R*,*R*/*S*,*S* form by single crystal X-ray diffraction analysis, was obtained as blocky crystals while the *meso* form was isolated as thin needles. Physical separation of the *R*,*R*/*S*,*S* diastereomeric pair facilitated the full assignment of the NMR spectra. The ^{31}P NMR spectrum displays only a single resonance at 30.4 ppm, but the ^1H and ^{13}C NMR spectra distinguish the *rac* and *meso* forms. The methine ^1H and ^{13}C resonances for H_5 and C_5 in $\mathbf{10_N}$ appear at δ 4.30, J_{HP} =13.1 Hz (*rac*), δ 4.14, J_{HP} = 13.1 Hz (*meso*), and δ 46.03, J_{CP} = 62.0 Hz (*rac*), δ 46.51, J_{CP} = 61.2 Hz (*meso*). The proton resonances are significantly upfield compared with the values for the methine proton resonances for $\mathbf{9_N}$ while the carbon resonances are slightly downfield of the shifts recorded for $\mathbf{9_N}$.

The oxidation of $\mathbf{8_N}$ was accomplished with peracetic acid, while the oxidation of $\mathbf{10_N}$ was performed with both peracetic

Scheme 2

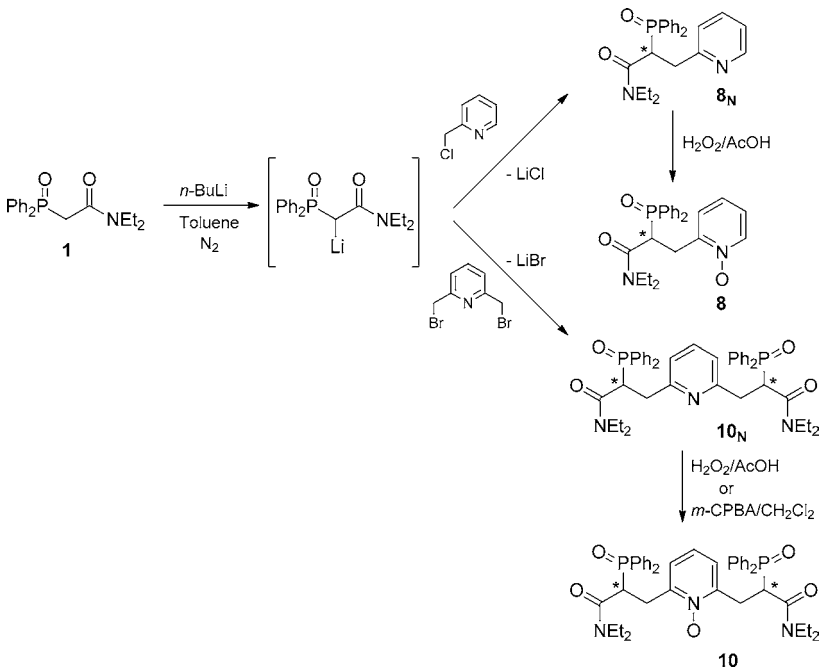

acid and *m*-CPBA. The resulting solid, white pyridine *N*-oxides were obtained as a racemic *R/S* mixture in 61% yield (**8**), and as a *rac/meso* 60/40 mixture (**10**) in 74% (peracetic acid) and 97% (*m*-CPBA) yields. The latter contained a low level impurity, as indicated by CHN analyses, that was not successfully removed. Small samples of diastereomerically pure **10** were obtained by oxidation of diastereomerically pure *rac* and *meso* samples of $\mathbf{10_N}$. The HRMS analyses of both **8** and **10** show high intensity [M + H$^+$] and [M + Na$^+$] ions. The FTIR spectrum for **8** displays absorptions centered at 1634, 1242, and 1180 cm^{-1} tentatively assigned to ν_{CO}, ν_{NO}, and ν_{PO}, respectively. The corresponding absorptions for **10** appear centered at 1632, 1253, and 1186 cm^{-1}. The ^{31}P NMR spectrum for **8** displays a single resonance at δ 32.0 ($CDCl_3$) or at δ 35.4 (d_4-MeOH) and the methine proton (H_7) and carbon (C_7) resonances appear at δ 4.79 (m) and 38.31 (J_{CP} = 62.6 Hz). On the other hand, the ^{31}P NMR spectrum for **10** contains two resonances, δ 32.5 (*rac*) and 30.8 (*meso*), and the methine proton (H_5) and carbon (C_5) resonances appear at δ 4.92 (*rac*), 4.83 (*meso*), and 39.33, J_{CP} = 62.0 Hz (*rac*), 38.89, J_{CP} = 63.3 Hz (*meso*).

The molecular structure of $\mathbf{8_R}$ was confirmed by single crystal X-ray diffraction techniques. A view of the molecule is provided in Figure 3, and selected bond lengths are listed in Table 3. The crystal used was obtained by slow evaporation of an acetone/EtOAc (80/20) solution of the racemic reaction product. There are two independent molecules in the unit cell, and both have the *R* configuration.[49] The pyridine *N*-oxide ring is planar, and the N−O bond vector is rotated away from the P═O and C═O bonds in the attached CMPO fragment. The P═O, C═O, and N−O bond lengths, 1.485 ± 0.004, 1.232 ± 0.001, and 1.314 ± 0.003 Å (av), respectively, are identical to the bond lengths in **7**. Several crystals of $\mathbf{10_N}$ were examined, but all gave X-ray diffraction data of marginal quality. Nonetheless, the composition was confirmed, and each crystal contained a racemic mixture of *R,R* and *S,S* enantiomers. Data from one crystal are deposited in the Supporting Information.

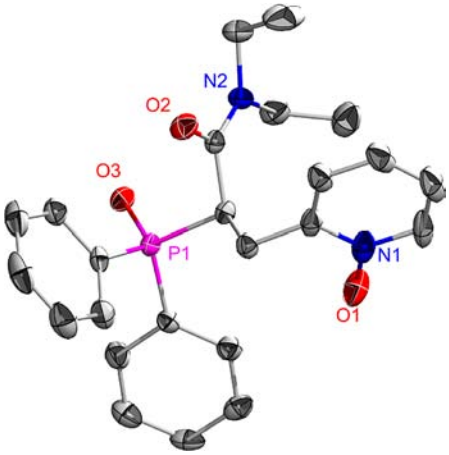

Figure 3. Molecular structure of (*R*)-{[$Ph_2P(O)$][C(O)NEt_2]C(H)-CH_2}C_5H_4NO, $\mathbf{8_R}$, (thermal ellipsoids, 50%) with carbon atom labels and H-atoms omitted for clarity.

Ligand Computational Modeling. The inclinations of these hybrid ligands to adopt maximal tridentate (**7** and **8**) and pentadentate (**9** and **10**) binding modes on a Ln(III) ion were evaluated by using a force field-based structure scoring approach described previously.[21h] The objective involves discovery of structures produced in gas phase metal ion coordination events that have low conformational energy, low degrees of induced strain, and few restricted bond rotations. The calculated values for the relative strain free energy (*G*) per bonded donor group in **7** (2.86 kcal/mol/donor group) and **8** (2.81 kcal/mol/donor group), wherein the donor groups are identical within the set, suggest that the NOPOCO ligands would both be expected to behave as tridentate chelators. Views of the calculated complexed forms of **7** and **8** are shown in Figure 4. Although the difference is small, the values of *G* per donor group suggest that the "floppier" ligand, **8**, that would utilize larger eight-membered chelate rings, should produce slightly more stable complexes compared to **7**. In contrast, the less "floppy" NOPOP′O′COC′O′ ligand, **9**, has smaller values of strain free energy per donor group than **10** when forming pentadentate chelate structures: $\mathbf{9_{R,R/S,S}}$, 4.33 kcal/mol/donor group, $\mathbf{9_{R,S}}$, 4.44 kcal/mol/donor group; $\mathbf{10_{R,R/S,S}}$, 4.54 kcal/mol/donor group, $\mathbf{10_{R,S}}$, 5.14 kcal/mol/donor group. Views of the pentadentate chelate structures are shown in Figure 5.

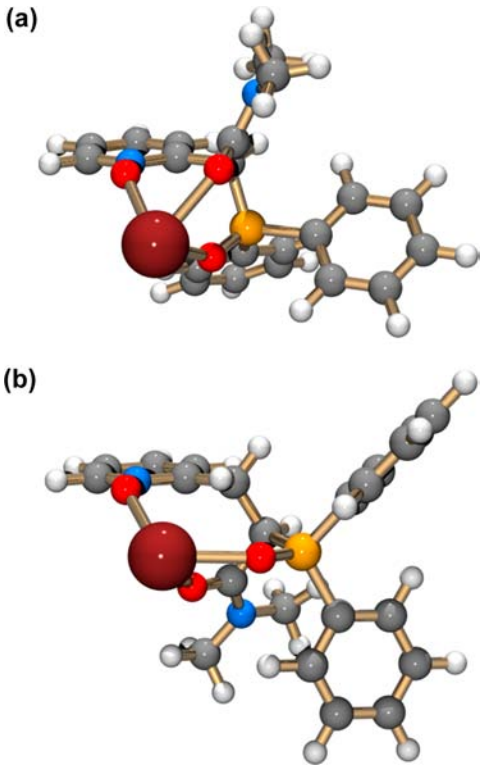

Figure 4. Geometry optimized structures for tridentate coordination in 1:1 ligand/Pr(III) complexes: (a) ligand **7**, (b) ligand **8**.

Although this steric analysis suggests that the maximum chelating conditions for **7** and **8** (tridentate) and **9** and **10** (pentadentate) should be accessible without serious ligand strain on a naked Ln(III) cation, the impact of inner sphere charge compensating anions (nitrate ions in particular) is ignored. The steric component of anion inclusion in the inner coordination sphere can be addressed in part by analysis of existing lanthanide structural data in the Cambridge Structural Database.[50] From a total of 758 structures of lanthanide complexes, $Ln(L)_n(NO_3)_3$, that contain three bidentate nitrate anions and ligands L that provide additional O-donor atoms in the inner coordination sphere, a plot of the number of additional O-donor atoms versus Shannon lanthanide ionic

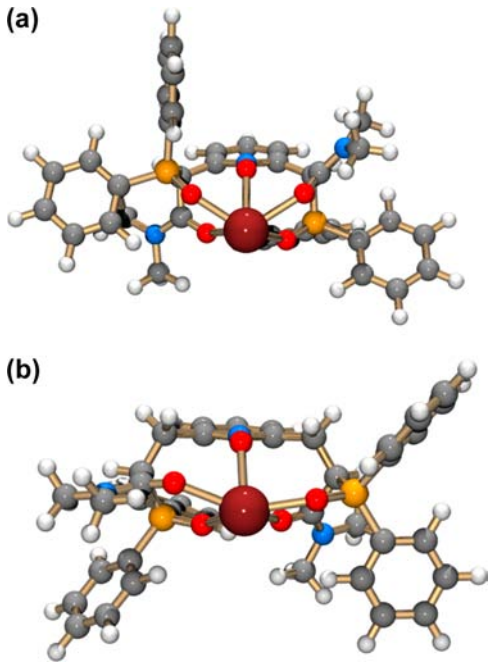

Figure 5. Geometry optimized structures for pentadentate coordination in 1:1 ligand/Pr(III) complexes: (a) ligand $\mathbf{9}_{R,R/S,S}$, (b) ligand $\mathbf{10}_{R,R/S,S}$.

radii (CN = 9) can be derived, and this plot is shown in Figure 6. The mean number of additional inner sphere O-atoms

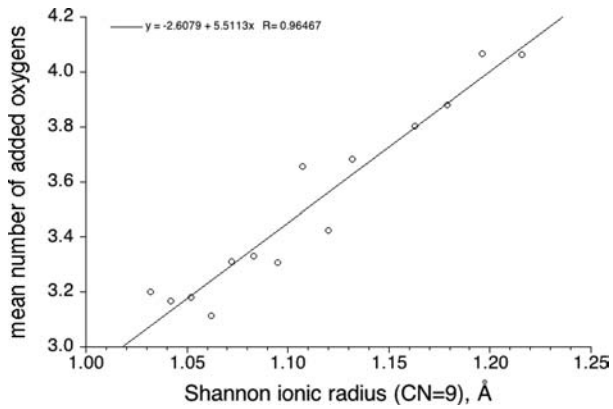

Figure 6. Plot of mean number of added ligand O-atoms vs Shannon ionic radii (Å) for Ln(III) ions (CN = 9).

reflects the amount of steric volume available on the lanthanide ion surface. This, in turn, parallels the size of the ion. If the mean donor atom number is less than 3.5, it is more commonly observed that three extra O-donor atoms are provided by the ligand(s) L, while if the mean donor atom number exceeds 3.5, four or more extra O-donor atoms are provided by the ligand(s). As expected, the latter condition is typically found for lanthanide ions larger than Gd(III). This analysis is consistent with the prediction that ligands **7** and **8**, each with three available O-donor atoms, should be able to employ all three to form tridentate NOCOPO chelate structures on any Ln(III) cation. Ligands **9** and **10** will likely form tridentate chelate structures on smaller, later lanthanide ions, due primarily to the limited available Ln(III) surface area, but tetradentate and perhaps pentadentate chelate structures may appear with the larger, early Ln(III) ions. Further, on the basis of limited data, it would be expected that the relative order of O-donor atom base strength would be $O_P \gg O_N > O_C$, so tridentate chelate structures involving **9** and **10** will likely utilize asymmetric NOPOP′O′ docking arrangements while the tetradentate and pentadentate structures will add one or two amide carbonyl O-atoms to the inner sphere environment. In order to test these predictions, the coordination chemistry of **7**−**10** was explored.

Lanthanide Ion Coordination Chemistry: One-Armed Ligands. Equimolar combinations of the one-armed ligands *rac*-**7** with $Ln(NO_3)_3{\cdot}x(H_2O)$ (Ln = La, Pr, Tb, Er) and *rac*-**8** with $Ln(NO_3)_3{\cdot}x(H_2O)$ (Ln = La, Pr, Eu, Dy, Er) in MeOH led to isolation of 1:1 complexes as solid powders. Elemental analyses of the powders are consistent with the 1:1 composition $[Ln(L)(NO_3)_3]$, although best agreement requires addition of water or MeOH as solvate molecules. For example, the CHN analyses for the Pr(III) complexes support the compositions $[Pr(\mathbf{7})(NO_3)_3]{\cdot}4H_2O$ and $[Pr(\mathbf{8})(NO_3)_3]{\cdot}MeOH$, and the presence of lattice solvent molecules is consistent with FTIR spectra. Solution ^{31}P NMR analyses for most of the complexes generally produce broad resonances due to lanthanide paramagnetic effects; however, spectra for diamagnetic La(III) complexes display sharp resonances. The ^{31}P NMR spectrum for crude $[La(\mathbf{7})(NO_3)_3]$ in d_4-MeOH contains a single resonance, δ 35.8, shifted downfield from the free ligand in d_4-MeOH, δ 31.6. Addition of a second equivalent of **7** provides a ^{31}P NMR spectrum with a single resonance, δ 34.6. Whether this small shift, relative to the 1:1 complex, indicates formation of a 2:1 complex in solution or simply rapid ligand exchange is not certain. All attempts to isolate a 2:1 complex were unsuccessful. The ^{31}P NMR spectrum for crude $[La(\mathbf{8})(NO_3)_3]$ in d_4-MeOH also displays a single resonance, δ 40.0, shifted downfield from the free ligand in d_4-MeOH, δ 35.4. Once again, addition of a second equivalent of **8** results in a small upfield shift relative to the shift for the 1:1 complex, δ 38.4, and efforts to isolate a 2:1 complex of **8** were unsuccessful. Shifts of the infrared stretching frequencies ν_{CO}, ν_{NO}, and ν_{PO} for the solid complexes in KBr relative to the free ligands provide some additional clues regarding the interactions of **7** and **8** with $Ln(NO_3)_3$ fragments. However, it must be noted that assignments for the bands are tentative especially for ν_{NO} which is of only modest intensity and falls in a region containing several other absorptions. The spectrum for the crude 1:1 complex $[Pr(\mathbf{7})(NO_3)_3]$ shows coordination shifts $\Delta\nu_{CO}$ = 36 cm^{-1}, $\Delta\nu_{NO}$ = 54 cm^{-1}, and $\Delta\nu_{PO}$ = 58 cm^{-1}, and these shifts are consistent with all three O-atom donors participating in the coordinate interaction. Similar shifts appear for the related complexes formed with the other Ln(III) ions. For $[Pr(\mathbf{8})(NO_3)_3]$, the coordination shifts are $\Delta\nu_{CO}$ = 33 cm^{-1}, $\Delta\nu_{NO}$ = 15 cm^{-1}, and $\Delta\nu_{PO}$ = 29 cm^{-1}. These data also are consistent with a tridentate, albeit weaker, chelate interaction between **8** and Pr(III).

Crystal Structure Analyses: One-Armed Ligand Complexes. Single crystals for one of the complexes containing **7** were obtained by dissolution of crude $[Pr(\mathbf{7})(NO_3)_3]{\cdot}4H_2O$ in acetone/ethyl acetate solution followed by slow evaporation of the homogeneous solution. The crystal structure determination reveals a composition for the single crystals as $[Pr(\mathbf{7}_R)(NO_3)_3(Me_2CO)]$. A view of the molecule is shown in Figure 7, and selected bond lengths are summarized in Table 4. The Pr(III) ion inner coordination sphere environment (CN = 10) is generated by three O-atoms from a tridentate ligand **7** in the *R* conformation, six O-atoms from three bidentate nitrate ions, and an O-atom provided by an acetone molecule. Although the

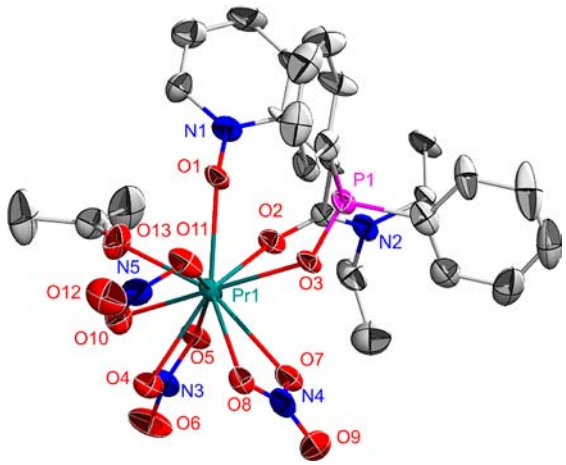

Figure 7. Molecular structure and atom labeling scheme for $[Pr(7_R)(NO_3)_3(Me_2CO)]$ (thermal ellipsoids, 50%) with carbon atom labels and H-atoms omitted for clarity.

phosphine oxide is generally considered to provide a significantly more basic donor O-atom, the Pr−O bond lengths involving **7** are remarkably similar: Pr1−O3(P) 2.457(7) Å, Pr1−O1(N) 2.479(8) Å, and Pr1−O2(C) 2.448(8) Å. In addition, the P═O, N—O, and C═O bond lengths in the complex, 1.502(8), 1.320(12), and 1.258(13) Å, respectively, are all elongated compared to the average bond lengths in the free ligand. These parameters are consistent with the IR coordination shifts observed for the crude complex. Similarly, a complex, $[Pr(\mathbf{5})_2(NO_3)_3]$, containing the related bifunctional NOPO ligand (**5**) (X = $CH_2P(O)Ph_2$), displays average Pr−O(P) and Pr−O(N) bond lengths of 2.457(6) and 2.446(6) Å, respectively.[31a] A structure for a CMPO/Pr(III) complex is not available for direct comparison, but the average Nd—O(P) and Nd—O(C) bond lengths in $\{Nd[Ph_2P(O)CH_2C(O)NEt_2](NO_3)_3\}$ are 2.457(4) and 2.493(4) Å, respectively.[18b] It is also of interest to compare the tridentate ligand binding mode displayed by **7** with the unexpected chelation interaction found between Pr(III) and the NOPOPO-type ligand $[Ph_2P(O)][Ph_2P(O)CH_2CH_2]C(H)C_5H_4NO$. In this case, the *N*-oxide O-atom and the *long-arm* phosphine oxide substituent's O-atom generate a bidentate chelate interaction while the short-arm phosphine oxide substituent forms a bridging interaction with another molecular unit.[31j]

The structure determination for single crystals recovered by slow evaporation of a solution containing the 1:1 combination of *rac*-**8** with $Pr(NO_3)_3{\cdot}6H_2O$ in MeOH unexpectedly reveals formation of a 1D polymeric structure. The repeating unit is shown in Figure 8, and selected bond lengths are listed in Table 4. Each Pr(III) ion is 10 coordinate with the coordination positions occupied by the O-atoms from a *bidentate* POCO chelating fragment of a $\mathbf{8}_R$ ligand, the O-atom of a pyridine *N*-oxide fragment of a second ligand molecule of opposite configuration, $\mathbf{8}_S$, the O-atoms of three bidentate nitrate ions, and the O-atom of an inner sphere molecule of MeOH. This provides an empirical formula, $[Pr(\mathbf{8}_R)(NO_3)_3(MeOH)-Pr(\mathbf{8}_S)(NO_3)_3(MeOH)]_n$, that is consistent with the CHN analytical data for the crude complex. The bridge linkage of the units occurs through the pyridine *N*-oxide O-atom. It is noteworthy that the average M-O(P) distance, 2.446 ± 0.001 Å, is the same as in the complex $[Pr(7_R)(NO_3)_3(Me_2CO)]$, but the average Pr−O(C) distance, 2.471 ± 0.007 Å is longer and the average Pr−O(N) distance is shorter, 2.435 ± 0.007 Å, than the respective distances in $[Pr(7_R)(NO_3)_3(Me_2CO)]$. Each of the P═O, N—O, and C═O bond lengths in the complex are elongated compared to the distances in the free ligand as expected with involvement of each donor site in the binding mode.

Lanthanide Ion Coordination Chemistry: Two-Armed Ligand 9. Equimolar combinations of the two-armed ligands **9** (*rac*/*meso* 54/46) with $Ln(NO_3)_3{\cdot}x(H_2O)$ (Ln = La, Pr, Nd, Eu, Dy, Er, Yb) in MeOH for two hours at 23 °C produced 1:1 complexes that were isolated as powders following evaporation of the volatiles. Characterization data for the crude complexes with Pr(III) are described as illustrative of these samples. Elemental analysis (CHN) data for the crude Pr(III) complex with **9** are most consistent with the formula $[Pr(\mathbf{9})(NO_3)_3]{\cdot}4H_2O$. An electrospray ionization mass spectrum for the related complex, $\{[Eu(\mathbf{9})(NO_3)_3]{\cdot}(Me_2CO)_{0.75}(H_2O)_{0.3}\}_4$, following its dissolution in MeOH and d_4-MeOH and use in photophysical studies, *vide infra*, shows a second most intense peak at 998.1834 amu corresponding to $[Eu(\mathbf{9})(NO_3)_2]^+$ consistent with a 1:1 ligand/metal composition. The peak and matching isotope pattern are shown in Supporting Information (Figure S.66). The most intense peak at 973.0988 amu corresponds to a species containing **9**, one Eu(III) ion, two methoxy anions, and two water molecules, $[Eu(\mathbf{9})(OCH_3)_2]^+{\cdot}H_2O{\cdot}HDO$ (Figure S.67, Supporting Information). The FTIR spectrum for the solid $[Pr(\mathbf{9})(NO_3)_3]{\cdot}4H_2O$ shows bands at 1637, 1612, 1246, and 1148 cm^{-1}. These are tentatively assigned to uncoordinated CO, coordinated CO, coordinated NO, and coordinated PO stretching modes, respectively. The coordination shifts, $\Delta\nu_{CO}$ = 6 cm^{-1}, $\Delta\nu_{CO}$ = 31 cm^{-1}, $\Delta\nu_{NO}$ = 29 cm^{-1}, and $\Delta\nu_{PO}$ = 55 cm^{-1}, are consistent with **9** acting as a tetradentate, NOPOPOCO ligand with one of the two amide carbonyl O-atoms not involved in the chelate interaction. The spectrum remains unchanged for samples obtained from reactions performed in MeOH at 23 °C for 12 h, in refluxing MeOH or acetone for two hours or for single crystals obtained from acetone/MeOH (4/1) mixtures. The same band patterns, with slight frequency differences, are obtained for La, Nd, and Eu complexes. The infrared spectrum of the residue obtained from a 1:1 combination of **9** with $Er(NO_3)_3{\cdot}5H_2O$ in MeOH (23 °C, 2 h) contains bands at 1244 and 1161 cm^{-1} that are tentatively assigned to NO and PO stretching vibrations, as well as a broader, more asymmetric band in the carbonyl region, 1660−1580 cm^{-1}, with a maximum at 1614 cm^{-1}. The last absorption is consistent with at least one of the carbonyl O-atoms participating in ligand binding. Crystallization of the crude Er(III) complex by slow evaporation of a acetone/ethyl acetate (4/1) solution produced two crystal morphologies (rectangular prisms and diamond-like plates) that were separated by hand. The rectangular prisms display an IR spectrum similar to the crude material with a broad ν_{CO} band centered at 1614 cm^{-1} that is consistent with carbonyl O-atom involvement in ligand coordination. On the other hand, the spectrum for the diamond-like crystals shows a single ν_{CO} band centered at 1649 cm^{-1} ($\Delta\nu_{CO}$ = −6 cm^{-1}). This single, up-frequency shifted CO vibration suggests that neither amide carbonyl O-atom of **9** is involved in coordination with the Er(III) ion; therefore, in this case the ligand is likely behaving only as a tridentate NOPOP′O′ chelate. Similar observations are also made for samples containing Dy(III) and Yb(III) ions.

Photophysical Characterization. Europium(III) is an emissive ion, due to metal-centered f−f transitions. Therefore,

Table 4. Selected Bond Lengths for Coordination Complexes (Å)

$[Pr(\mathbf{7}_R)(NO_3)_3(Me_2CO)]$	$[Pr(\mathbf{8}_R)(NO_3)_3(MeOH)$-$Pr(\mathbf{8}_S)(NO_3)_3(MeOH)]_n$	$\{[Eu(\mathbf{9}_{R,S})(NO_3)_3]\cdot(Me_2CO)_{0.75}\cdot(H_2O)_{0.3}\}_4$	$[Pr(\mathbf{9}_{R,S})(NO_3)_3]$	$[Er(\mathbf{9}_{R,S})(NO_3)_3]\cdot Me_2CO$	$[Er(\mathbf{9}_{S,S})(NO_3)_2(H_2O)](NO_3)\cdot(MeOH)\cdot(H_2O)_{0.4}$	$\{[Pr(\mathbf{10}_{R,S})(NO_3)(H_2O)]_2(\mu\text{-}\mathbf{10}_{R,R})\}(NO_3)_4$
M−O(P) Bond						
Pr1−O3 2.457(7)	Pr1−O5#2 2.446(6)	Eu1−O3 2.433(4)	Pr1−O10 2.415(2)	Er1−O2 2.300(2)	Er1−O2 2.283(2)	Pr1−O3 2.426(4)
	Pr2−O2 2.447(6)	Eu1−O5 2.354(4)	Pr1−O13 2.478(2)	Er1−O4 2.293(2)	Er1−O4 2.310(2)	Pr1−O5 2.492(4)
						Pr1−O8 2.478(4)
$M-O(N)_{pyr}$ Bond						
Pr1−O1 2.479(8)	Pr1−O1 2.442(6)	Eu1−O1 2.467(3)	Pr1−O12 2.513(2)	Er1−O1 2.321(2)	Er1−O1 2.466(2)	Pr1−O1 2.452(4)
	Pr2−O4 2.427(6)					
M−O(C) Bond						
Pr1−O2 2.448(8)	Pr1−O6#2 2.464(6)	Eu1−O2 2.435(4)	Pr1−O14 2.470(2)		Er1−O5 2.310(2)	Pr1−O4 2.482(4)
	Pr2−O3 2.478(7)					Pr1−O2 2.589(4)
$M-O_{nitrate}$						
av 2.58 ± 0.02	av 2.62 ± 0.05[a]	av 2.54 ± 0.05	av 2.60 ± 0.03	av 2.43 ± 0.03	av 2.44 ± 0.01	av 2.588(4)
range 2.549(9)−2.615(10)	range 2.577(9)−2.757(7)[a]	range 2.497(4)−2.613(4)	range 2.572(2)−2.639(2)	range 2.399(2)−2.480(2)	range 2.428(2)−2.460(2)	
$M-O_{(solv)}$ Bond						
Pr1−O13 2.524(8)	Pr1−O25 2.552(7)				Er1−O15 2.288(2)	Pr1−O15 2.475(5)
	Pr2−O26 2.540(7)					
P−O Bond						
P1−O3 1.502(8)	P1−O2 1.507(7)	P1−O3 1.503(3)	P1−O10 1.500(2)	P1−O2 1.506(2)	P1−O2 1.497(2)	P1−O3 1.503(4)
	P2−O5 1.506(6)	P2−O5 1.505(4)	P2−O13 1.495(2)	P2−O4 1.507(2)	P2−O4 1.496(2)	P2−O5 1.506(4)
						P3−O8 1.498(4)
N−O Bond						
N1−O1 1.320(12)	N1−O1 1.329(9)	N1−O1 1.328(5)	N5−O12 1.327(3)	N1−O1 1.335(3)	N1−O1 1.313(3)	N1−O1 1.327(6)
	N3−O4 1.328(10)					N4−O6 1.324(9)
C−O Bond						
C7−O2 1.258(13)	C8−O3 1.270(11)	C7−O2 1.263(6)	C31−O14 1.250(4)	C7−O3 1.230(4)	C25−O5 1.252(3)	C8−O2 1.236(8)
	C32−O6 1.263(12)	C25−O4 1.236(7)	C8−O11 1.237(4)	C25−O5 1.232(4)	C7−O3 1.236(3)	C27−O4 1.242(7)
						C49−O7 1.220(7)

[a]Disordered nitrate O-atoms excluded.

dx.doi.org/10.1021/ic3025342 | Inorg. Chem. 2013, 52, 3063−3083

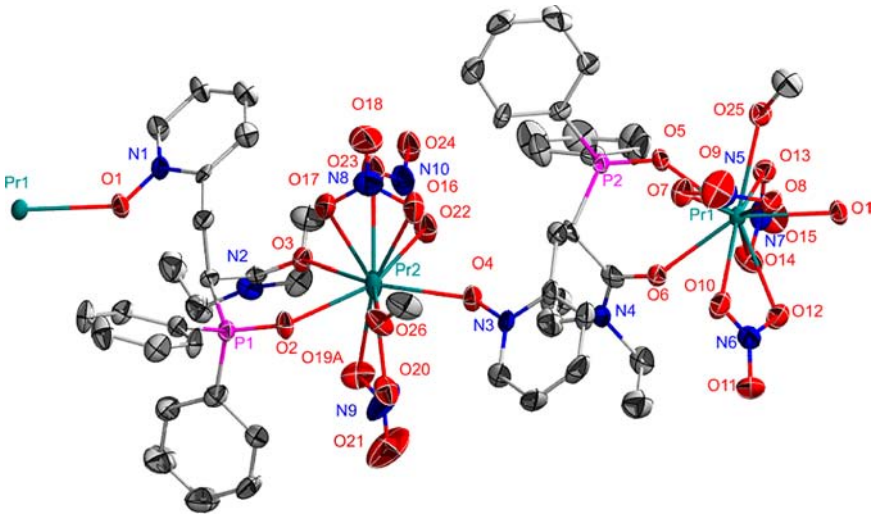

Figure 8. Molecular structure and atom labeling scheme for $[Pr(\mathbf{8}_R)(NO_3)_3(MeOH)-Pr(\mathbf{8}_S)(NO_3)_3(MeOH)]_n$ (thermal ellipsoids, 50%) with carbon atom labels and H-atoms omitted for clarity.

in order to gain additional structural information, the emission spectroscopy of the Eu(III) complex of **9** was examined in the solid state and in methanol solution. The emission spectrum for the crystallographically characterized solid,$\{[Eu(\mathbf{9})(NO_3)_3]\cdot(Me_2CO)_{0.75}(H_2O)_{0.3}\}_4$, *vide infra*, is shown in Figure 9a, and the spectrum for $[Eu(\mathbf{9})(NO_3)_3]$ in methanol is presented in Figure 9 b. The spectra are similar, and contain the characteristic emission peaks of Eu(III) centered at 579, (591) 594, 614, 617, 649, (685) 689, and (696) 700 nm (solid) and 579, 590, 613, 648, and 691 nm (MeOH solution). These correspond to the $^5D_0 \rightarrow {}^7F_J$ (J = 0, 1, 2, 3, 4) transitions. The appearance and intensities of the transition to the J = 0 ground state and the electric dipole forbidden transition to J = 2 are consistent with the absence of an inversion center in the complex. A spectrum obtained from a frozen (77 K) methanol solution shows splitting of the J = 1 transition into at least three components and the J = 2 transition into at least three, possibly up to five, components. This additionally indicates a low symmetry environment around the metal ion. Following the method of descending symmetry, such splitting is consistent with the point groups C_1, C_s, C_2, and C_{2v}.[51] This spectrum is distinct from the one obtained from the solid sample (Figure 9 a) indicating that the structure in the frozen methanol solution is different from the solid structure. Attempts to compare the emission spectrum at 77 K with the one from the solution at room temperature showed similar broadening of the peaks. However, due to low resolution, the peak splittings were not observed. To further clarify the room-temperature solution structure of the metal center, the emission lifetime of Eu(III) in methanol, 0.3627 ± 0.0388 ms (Figure S.68, Supporting Information), and in deuterated methanol, 1.2743 ± 0.1073 ms (Figure S.69, Supporting Information), were compared by using the Horrocks' equation.[40] This indicates that four methanol solvent molecules replace the three nitrate anions in solution, maintaining a low symmetry environment around the metal ion.

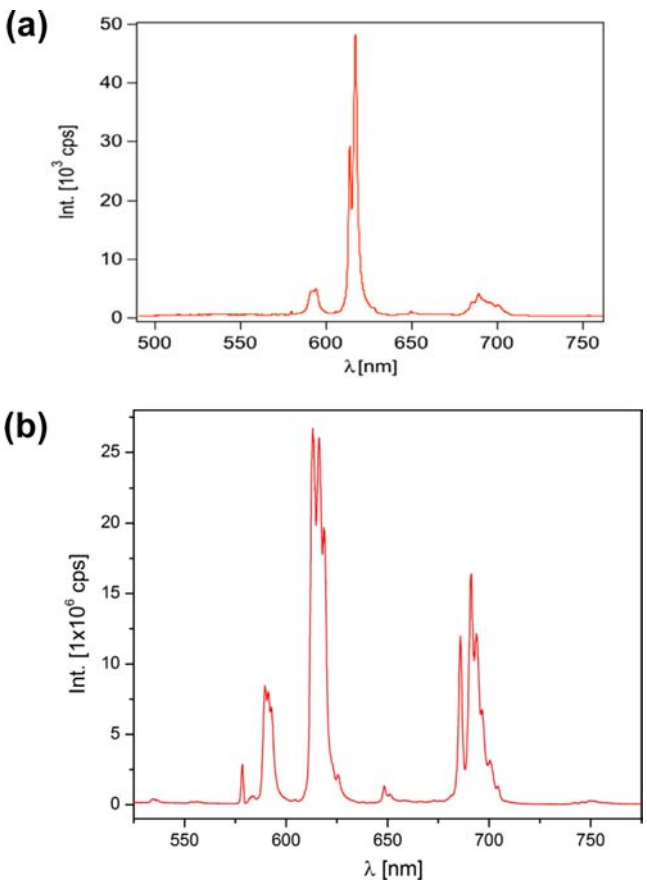

Figure 9. Emission spectrum of (a) $\{[Eu(\mathbf{9})(NO_3)_3](MeOH)(H_2O)$ (crystalline solid), λ_{exc} = 488 nm, 1 μW, and (b) $[Eu(\mathbf{9})(NO_3)_3]$ in methanol (77 K). λ_{exc} = 289 nm.

Lanthanide Ion Coordination Chemistry: Two-Armed Ligand 10. Equimolar combinations of the two-armed ligand **10** (*rac*/*meso* 60/40) with $Ln(NO_3)_3\cdot x(H_2O)$ (Ln = La, Pr, Eu, Dy, Er) in MeOH for two hours at 23 °C gave powder samples following evaporation of the volatiles. Characterization data for the crude complex with Pr(III) are described as illustrative of these samples. Interpretation of the analytical data for this complex was initially unclear. However, following a X-ray structure determination for crystals obtained by crystallization of the crude complex from MeOH/acetone, *vide infra*, a composition corresponding to $[Pr_2(\mathbf{10})_3(NO_3)_6(H_2O)_2]\cdot 12H_2O$ was suggested, and found to be in good agreement with the analytical data. The infrared spectrum obtained from

the crude Pr(III) complex with **10** displays bands centered at 1601, 1213, and 1155 cm^{-1} assigned to CO, NO, and PO stretching modes, respectively. These correspond to coordination shifts of $\Delta\nu_{CO}$ = 31 cm^{-1}, $\Delta\nu_{NO}$ = 40 cm^{-1}, and $\Delta\nu_{PO}$ = 31 cm^{-1}. It is noted that the band assigned to the carbonyl stretch in this complex is roughly doubled in width compared to the width of the band assigned to the CO stretching mode for the free ligand. This may indicate that there are overlapping bands for coordinated and uncoordinated amide carbonyl groups. Supporting this conclusion, an IR spectrum for single crystals of the complex containing Pr(III) and **10** shows two resolved carbonyl frequencies centered at 1620 and 1597 cm^{-1}. Similar band patterns and frequencies are observed for the La, Eu, Dy, and Er complexes of **10**.

Crystal Structure Analyses: Two-Armed Ligand Complexes. The spectroscopic data outlined above support the conclusion that **9** and **10** act as chelating ligands toward Ln(III) ions, but the detailed nature of the ligand/lanthanide interactions in both solution and the solid state remained unclear. As a result, single crystal X-ray diffraction analyses were undertaken for six complexes of **9** and one of **10**. For the crystalline complexes of **9**, the starting materials were the crude powders obtained from the equimolar combinations of **9** (*rac*/*meso* 54/46) and $Ln(NO_3)_3{\cdot}6H_2O$ in MeOH (23 °C, 2 h). The crude complexes were dissolved in a minimum of acetone/MeOH (4/1) and the solutions allowed to slowly evaporate whereupon suitable single crystals for the Pr(III) and Eu(III) complexes were obtained. The structures appear to be isomorphous although difficulty was encountered with the refinement of the outer sphere solvent atoms in both complexes. The refinement for the Eu(III) complex leads to an empirical formula $\{[Eu(\mathbf{9}_{R,S})(NO_3)_3]{\cdot}(Me_2CO)_{0.75}{\cdot}(H_2O)_{0.3}\}_4$ in which the solvent void volume is not fully ordered and occupied. A suitable disorder model was not found for the Pr(III) complex, so in this case the SQUEEZE procedure was applied. Views for $\{[Eu(\mathbf{9}_{R,S})(NO_3)_3]{\cdot}(Me_2CO)_{0.75}{\cdot}(H_2O)_{0.3}\}_4$ and $[Pr(\mathbf{9}_{R,S})(NO_3)_3]$ are shown in Figures 10 and 11, and selected bond lengths are provided in Table 4. In both cases the Ln(III) ion is bonded to three bidentate nitrate anions and one neutral, *meso*, tetradentate ligand, $\mathbf{9}_{R,S}$, in which the NOPOP′O′CO chelate interaction is asymmetric with one amide (*S* conformer arm) coordinated to the Ln(III) and the second amide arm (*R* conformer arm) rotated away from the Ln(III) center. The ligand docking asymmetry is also indicated by significantly different Pr−O(P) bond lengths: Pr1−O10 2.415(2) Å and Pr1−O13 2.478(2) Å; a similar asymmetry pattern is found in the Eu(III) complex. The Pr−O(N) distance, Pr1−O12, 2.513(2) Å, is notably longer as often observed with tridentate complexes of **6** (X = $CH_2P(O)Ph_2$).[31] The Pr−O(C) bond length, Pr1−O14, 2.470(2) Å, is comparable to the distances in the Pr(III) complexes of **7** and **8** described earlier. It is noted that the asymmetric tetradentate chelate interactions observed in the crystal structures are consistent with the IR data recorded from KBr pellets for these early lanthanide ion complexes, and with the emission spectroscopic data for the solid and methanol solutions of the Eu(III) complex, *vide supra*.

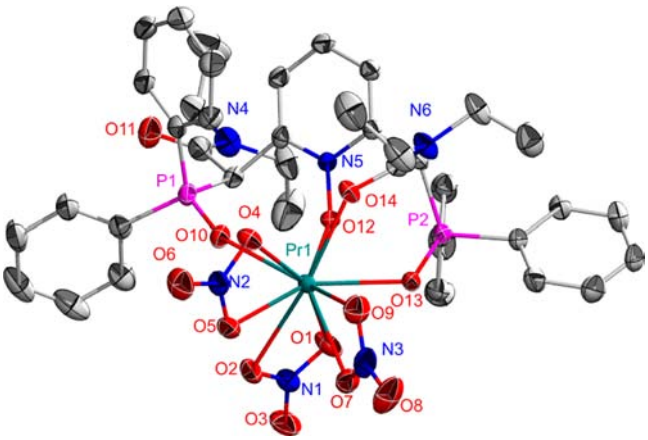

Figure 11. Molecular structure and atom labeling scheme for $[Pr(\mathbf{9}_{R,S})(NO_3)_3]$ (thermal ellipsoids, 50%) with carbon atom labels, H-atoms, and outer sphere solvent molecules omitted for clarity.

Interestingly, as mentioned above, crystallization by slow evaporation of a acetone/ethyl acetate (4/1) solution of the crude complex of **9** with $Er(NO_3)_3$ provided crystals with two different morphologies: diamond-like plates and rectangular prisms. The molecular structure obtained from the diamond-like crystals is shown in Figure 12, and selected bond lengths are presented in Table 4. The complex, $[Er(\mathbf{9}_{R,S})(NO_3)_3]{\cdot}(Me_2CO)$, contains a nine-coordinate Er(III) with the inner sphere coordination polyhedron generated by six O-

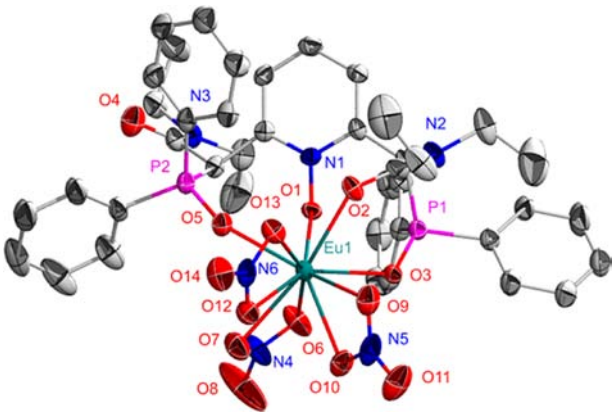

Figure 10. Molecular structure and atom labeling scheme for $\{[Eu(\mathbf{9}_{R,S})(NO_3)_3]{\cdot}(Me_2CO)_{0.75}{\cdot}(H_2O)_{0.3}\}_4$ (thermal ellipsoids, 50%) with carbon atom labels, lattice Me_2CO and H_2O, and H-atoms omitted for clarity.

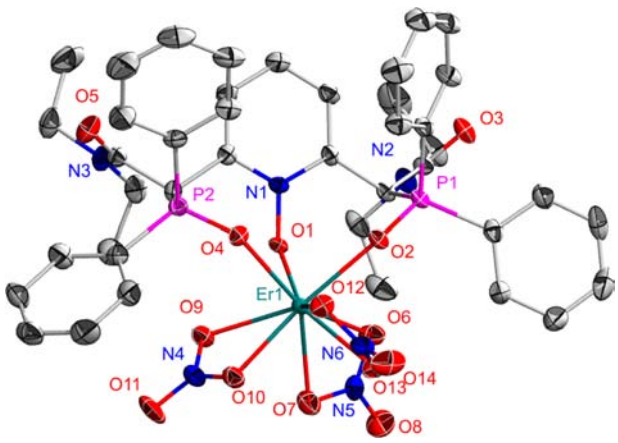

Figure 12. Molecular structure and atom labeling scheme for $[Er(\mathbf{9}_{R,S})(NO_3)_3]{\cdot}(Me_2CO)$ (thermal ellipsoids, 50%) with carbon atom labels, lattice Me_2CO, and H-atoms omitted for clarity.

atoms from three bidentate nitrate anions and three O-atoms provided by a neutral, tridentate NOPOP′O′ chelated ligand, **9**, in its *meso* form . Both amide carbonyl units are rotated away from the Er(III) ion coordination pocket, and they are not involved in the inner sphere coordination interaction. This tridentate chelation mode is consistent with the IR spectrum that shows a single strong, relatively sharp carbonyl stretch at 1647 cm^{-1} that is essentially unperturbed from the free ligand vibration, ν_{CO} =1643 cm^{-1}, *vide supra*. The ligand is symmetrically docked on the Er(III) as indicated by nearly equivalent Er−O(P) and Er−O(N) bond lengths: Er1−O2 2.300(2) Å, Er1−O4 2.293(2) Å, and Er1−O1 2.321(2) Å. In this sense, the ligand behaves much like the previously studied NOPOP′O′ ligands, **6**, [X = $CH_2P(O)PR_2$].[31] For example, the Er−O bond lengths can be compared with the distances in the related 1:1 complexes, [Er(**6**)$(NO_3)_3$] (X = $CH_2P(O)PPhBz$): Er−O(P) 2.280(7) and 2.281(7) Å and Er−O(N) 2.278(7) Å.[31h] For [Er(**6**)$(NO_3)_3$] (X = $CH_2P(O)Cy_2$), the distances follow: Er−O(P) 2.249(2) and 2.253(2) and Er−O(N) 2.318(2) Å.

The molecular structure determined from the rectangular prisms, on the other hand, revealed a different composition, [Er($\mathbf{9}_{S,S}$)$(NO_3)_2(H_2O)$](NO_3) ·(MeOH)·$(H_2O)_{0.4}$. A view of the complex is shown in Figure 13, and selected bond lengths

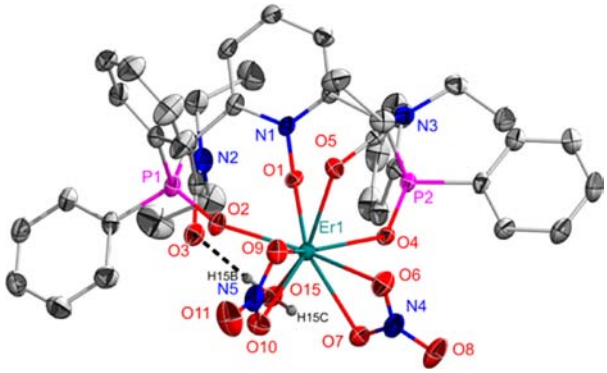

Figure 13. Molecular structure and atom labeling scheme for [Er($\mathbf{9}_{S,S}$)$(NO_3)_2(H_2O)$](NO_3)·(MeOH)·$(H_2O)_{0.4}$ (50% thermal ellipsoids) with carbon atom labels, outer-sphere nitrate ion, lattice solvents, and H-atoms except for inner sphere water molecule omitted for clarity.

are presented in Table 4. The central Er(III) is eight-coordinate with the coordination positions occupied by four O-atoms provided by *two* bidentate nitrate anions and four O-atoms from a neutral, *tetradentate*, NOPOP′O′CO-bonded ligand **9** in its *S,S* enantiomeric form. In contrast to the interactions of **9** with the early lanthanide ions Pr(III) and Eu(III), the free amide arm is not rotated away from the Er(III) ion. Instead, it points directly at and is hydrogen bonded with a H-atom of an Er(III)-bound water molecule with O15−H15B 0.77(3) Å, O3···H15B 1.92(3) Å, O15···O3 2.690(3) Å, and O3−H15B−O15 176.0°. The relevant bond lengths involving **9** and the Er(III) ion are Er−O(P), Er1−O2 2.283 (2) Å, and Er−O4 2.310(2) Å, Er−O(N) Er1−O1 2.466(2) Å, Er−O(C) Er1−O5 2.310(2) Å, and Er−O(H) Er−O15 2.288(2) Å. The donor group bond lengths in the ligand, P−O 1.497(2) and 1.496(2) Å, N−O 1.313(4) Å, and C−O 1.252(3) and 1.236(3) Å, are all elongated relative to the bond lengths in the free ligand. For the amide fragments, the greater C−O bond elongation occurs, as expected, for the carbonyl bonded to the Er(III) ion. This structure is consistent with the IR spectrum for the complex which displays a very broad absorption in the carbonyl stretch region.

The crude complexes formed by **9** and two other late lanthanides, Dy(III) and Yb(III), in MeOH solutions, following crystallization from acetone/ethyl acetate (4/1) solution, also provide crystals with two different morphologies (diamond-like and needles (Yb) or diamond-like and microcrystalline powder (Dy)). X-ray crystal structure determinations for both diamond-like crystals show that the complexes are isomorphous with the complex [Er($\mathbf{9}_{R,S}$)$(NO_3)_3$]·(Me_2CO). The relevant structural data are provided in Supporting Information. It is noted as well that these complexes display IR spectra that are nearly identical and each shows a relatively narrow, unperturbed ν_{CO} band, compared to the free ligand, consistent with tridentate coordination of **9**. Unfortunately, the needle crystalline form of the Yb(III) complex was not of sufficient quality to permit a X-ray structure determination; however, it is likely that the structure for this complex resembles the structure of [Er($\mathbf{9}_{S,S}$)$(NO_3)_2(H_2O)$](NO_3)·(MeOH)·$(H_2O)_{0.4}$ that contains a tetradentate chelated ligand **9**.

The molecular structure determination for the complex isolated from the equimolar combination of **10** and Pr-$(NO_3)_3$·$6H_2O$ in MeOH and crystallized from acetone/MeOH (4/1) solution provides an additional interesting result. A view of the structure is shown in Figure 14, and selected bond lengths are summarized in Table 4. The complex, {[Pr($\mathbf{10}_{R,S}$)-$(NO_3)(H_2O)$]$_2$(μ-$\mathbf{10}_{R,R}$)}$(NO_3)_4$, is composed of two [Pr-($\mathbf{10}_{R,S}$)$(NO_3)(H_2O)$] units, each containing a central Pr(III) ion bonded to one bidentate nitrate anion, a molecule of water, and an asymmetrically docked, *pentadentate* NOPOP′O′CO-C′O′ ligand, $\mathbf{10}_{R,S}$. The two equivalent fragments are bridged through Pr—O═P bonds by a third ligand molecule, $\mathbf{10}_{R,R}$. As a result, each Pr(III) is nine-coordinate. Four disordered nitrate counterions appear in the outer sphere, and these were treated through SQUEEZE. Four of the five Pr−O bond lengths involving the pentadentate ligand are relatively similar, Pr1−O3(P) 2.426(4) Å, Pr1−O5(P) 2.492(4) Å, Pr1−O1(N) 2.452(4) Å, Pr1−O4(C) 2.482(4) Å. The coordinate bond formed by the second amide carbonyl group is longer, Pr1−O2 2.589(4) Å, and more comparable to the bond lengths involving the inner sphere nitrate ion, Pr1−O9 2.589(4) and Pr1−O10 2.5888(4) Å. The bridging Pr1−O8(P) bond length, 2.478(4) Å, and the coordinated water distance, Pr1−O15, 2.475(5) Å, are similar to the shorter Pr−O bond lengths involving the pentadentate ligand. The functional group bond lengths are consistent with the coordination modes displayed by the ligand: N1−O1 1.327(6) Å, P1−O3 1.503(4) Å, P2−O5 1.506(4) Å, C8−O2 1.236(8) Å, C27−O4 1.242(7) Å, P3−O8 1.498(4) Å, C49−O7 1.220(7) Å. The unbound pyridine *N*-oxide bond length, N4−O6 1.324(9) Å, is somewhat longer than expected.

Solvent Extraction Analyses. The interesting lanthanide coordination chemistry displayed by **7**−**10** encouraged studies of the solvent extraction performance of the new hybrid ligands. The aryl derivatives described here are not appreciably soluble in the preferred organic diluent dodecane; however, each is readily soluble in 1,2-dichloroethane (DCE), and this diluent was used for initial screening extraction measurements. Distribution ratios, D = $[M_{org}]/[M_{aq}]$, were measured for Eu(III) and Am(III) in nitric acid solutions under identical conditions at 25 °C by using 0.01 M solutions of **7**−**10** in DCE. The variations of D values on nitric acid concentration for the

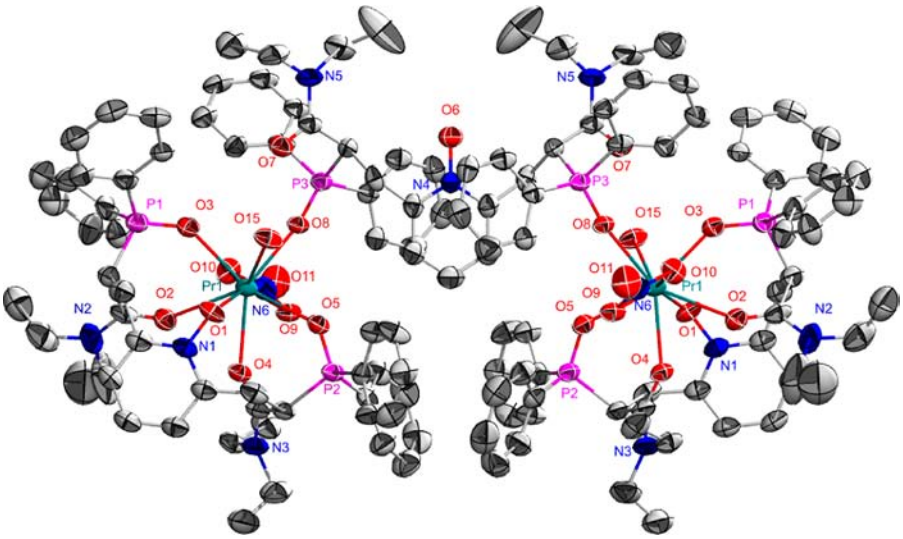

Figure 14. Molecular structure and atom labeling scheme for$\{[Pr(\mathbf{10}_{R,S})(NO_3)(H_2O)]_2(\mu\text{-}\mathbf{10}_{R,R})\}(NO_3)_4$ (50% thermal ellipsoids) with carbon atom labels, outer-sphere nitrate ions, and H-atoms omitted for clarity.

"one-armed" ligands **7** and **8**, as well as for OPhDiBCMPO, are shown in Figure 15. It is apparent that, at all nitric acid concentrations, **7** is a superior extractant compared to **8**, and OPhDiBCMPO is intermediate in performance between **7** and **8**. This result contrasts with the steric modeling prediction that the "floppier" ligand **8** would provide slightly smaller steric strain per donor group than **7**. Of course, additional factors beyond steric strain contribute to the magnitudes of *D* values. All three compounds show increasing *D* values for Eu(III) and Am(III) with increasing nitric acid concentration in the range 0.01−1 M. At higher acid concentrations, the *D* values decrease likely as a result of competing ligand protonation reactions. This behavior is also observed with CMPO, NOPO, and NOPOPO extractions.[13,16,32−35] In addition, each compound, at the same $[HNO_3]$, displays better extractions for Am(III) than for Eu(III) with the greatest differentiation occurring with **7**.

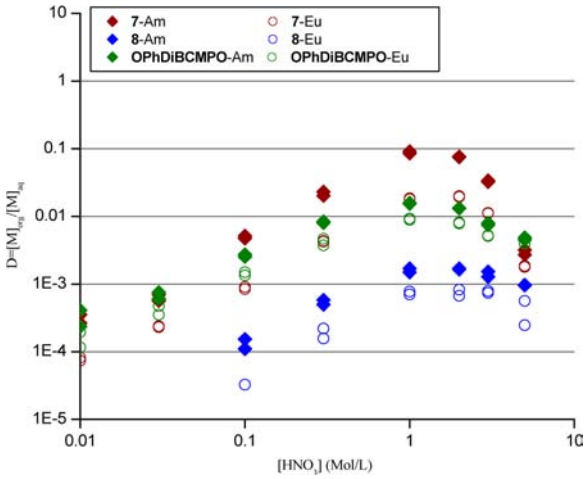

Figure 15. Americium and europium distribution ratios as a function of the initial nitric acid concentration. Organic phase: **7**, **8**, or OPhDiBCMPO at 10 mM in 1,2-DCE. Aqueous phase: trace ^{241}Am and 0.1 mM of europium nitrate in nitric acid. O/A = 1, *T* = 25 °C.

The dependencies of *D* values on nitric acid concentration for extractions with DCE solutions of the "two-armed" ligands **9** and **10** are displayed in Figure 16 along with data for OPhDiBCMPO and TONOPOPO measured under identical conditions. First, it is pointed out that although previous studies have indicated that the NOPOPO-class of extractants provides slightly improved performance relative to the CMPO-class extractants,[32−35] accurate comparisons have not been possible since the extraction data have not been obtained under identical experimental conditions. The data in Figure 16 provide for a direct evaluation albeit in a chlorocarbon solvent, DCE. At all initial nitric acid concentrations, the *D* values for TONOPOPO are significantly greater than the *D* values for OPhDiBCMPO. Further, it is observed that both compounds exhibit increasing *D* values with increasing initial nitric acid concentration from 0.01 to 0.3 M.[52] From 0.3 to 1 M $[HNO_3]$, the *D* values for TONOPOPO begin to decrease while the *D* values for

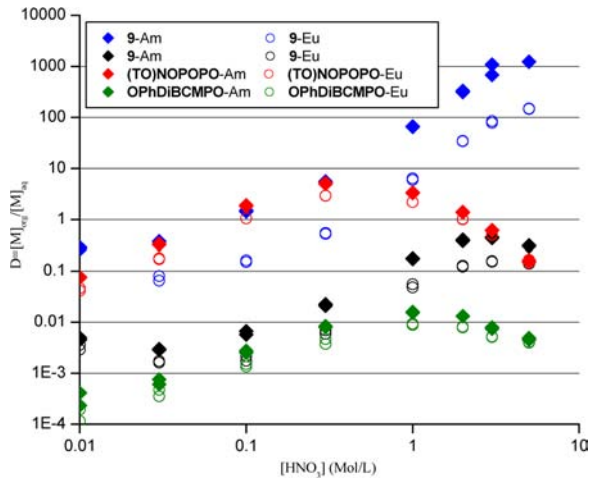

Figure 16. Americium and europium distribution ratios as a function of the initial nitric acid concentration. Organic phase: **9**, **10**, (TO)NOPOPO, or OPhDiBCMPO at 10 mM in 1,2-DCE. Aqueous phase: trace ^{241}Am and 0.1 mM of europium nitrate in nitric acid. O/A = 1, *T* = 25 °C.

OPhDiBCMPO continue to increase up to 1 M [HNO_3] and then decrease. In both cases, at all [HNO_3], the D values for Am(III) are slightly greater than for Eu(III). Extractions with **10** generally parallel the performance of OPhDiBCMPO in the initial acid range 0.01−0.3 M, but at higher acid concentrations the D values for **10** continue to increase up to 3 M [HNO_3] before declining at the highest acid concentrations. At all [HNO_3] up to 3 M the D values for **10** are significantly smaller than those observed with TONOPOPO. Furthermore, the D values for Am(III) are slightly greater than those for Eu(III) at all [HNO_3].

The particularly interesting observations appear in the extractions performed with **9**. Here, the D values are much greater than those for **10** or OPhDiBCMPO at all nitric acid concentrations. In the acid concentration range 0.01−0.3 M the D values for **9** and TONOPOPO extractions of Am(III) are essentially identical while the D values for **9** are smaller than for TONOPOPO extractions of Eu(III). However, above 1 M [HNO_3], **9** is a dramatically better extractant than TONOPOPO for both Am(III) and Eu(III), and the D values for both continue to increase up to at least 5 M [HNO_3]. For this case, the f-element cation very favorably competes against proton for the ligand donor sites. At all acid concentrations D_{Am} is significantly greater than D_{Eu}, and at 1 M [HNO_3] the separation ratio $D_{Am}/D_{Eu} \sim 10$. This separation factor is noticeably larger than typically encountered with many all-O-atom donor chelating extractants such as CMPO and NOPOPO, comparable with a few "calix-tethered"-CMPO extractants,[27b,j] but smaller than reported for several soft donor extractants.[5−7]

Lastly, ligand dependency analyses for extractions of Am(III) and Eu(III) by **9**, TONOPOPO, and OPhDiBCMPO in DCE, measured at 1 M [HNO_3] without correction for ligand protonation, are summarized in Figure 17. As expected, the

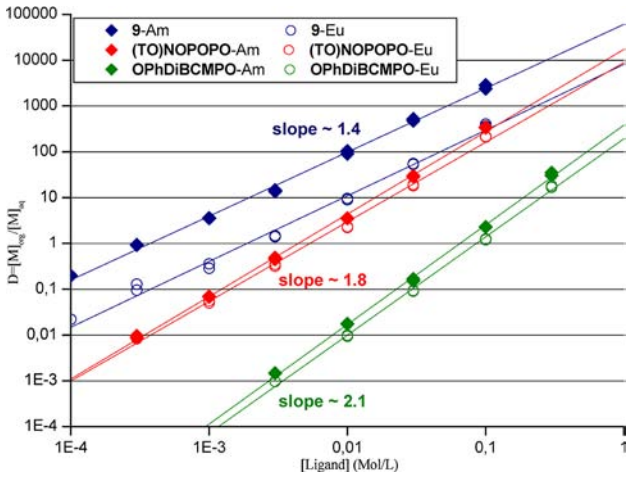

Figure 17. Dependence of distribution ratios D for Eu(III) and Am(III) on concentration of **9**, (TO)NOPOPO, and OPhDiBCMPO in DCE from 1 M HNO_3 at 25 °C.

ligand dependencies for Am(III) and Eu(III), with each ligand, are similar, and the slopes are ∼1.4, 1.8, and 2.1, respectively. These data suggest that the ligands probably form a combination of 1:1 and 2:1 ligand/metal complexes in DCE with the 1:1 stoichiometry most prevalent with **9**. This is consistent with the conclusion that asymmetric, tetradentate and perhaps pentadentate ligand/metal ion interactions persist under extraction conditions with **9** and likely with **10**.

■ CONCLUSION

Synthetic procedures have been successfully designed and implemented for the marriage of carbamolymethylphosphine oxide fragments to pyridine *N*-oxide and methylpyridine *N*-oxide platforms. Computational analyses of steric strain incurred by the ligands when adopting energy minimized, maximal multidentate docking interactions on Ln(III) ions indicate that the "one-armed" ligands, **7** and **8**, and the "two-armed" ligands, **9** and **10**, should be able to accommodate tridentate and pentadentate chelate binding modes, respectively. Selected coordination chemistry with lanthanide nitrates was surveyed, and several 1:1 complexes were isolated. Under the conditions explored, 2:1 complexes were not isolated although the formation of such species, with reduced ligand denticities, may well occur especially in noncoordinating organic solutions. Spectroscopic analyses suggest that the ligand docking interactions in organic solutions are asymmetric and hemilabile-like. Crystal structure analyses for complexes containing the "one-armed" ligands indicate that **7** adopts the tridentate NOPOCO chelate condition while **8** prefers to utilize a mixed bidentate POCO/bridging NO binding mode. Structures for complexes containing the "two-armed" ligands, **9** and **10**, not surprisingly, show greater diversity with examples of tridentate, tetradentate, and pentadentate binding. Initial solvent extraction screening using solutions of the ligands dissolved in DCE in contact with Eu(III) and Am(III) in aqueous nitric acid solutions reveal impressive performance for **7** and especially **9**. Stimulated by these results, more detailed spectroscopic studies of the ligand/Ln(III) coordination interactions in solution, additional crystallographic analyses of isolated coordination complexes, and expanded extraction analyses are in progress. The results from these studies, as well as parallel discoveries involving the development of related NOPOCO and NOPOPOCOCO ligands with attachments through the amide N-atom, will be reported separately.

■ ASSOCIATED CONTENT

Ⓢ Supporting Information

Selected IR, HRMS, emission and NMR spectra, summary of separation factors, and CIF data for the crystal structures. This material is available free of charge via the Internet at http://pubs.acs.org. X-ray data for $\mathbf{8}_R.\mathbf{8}_S$ have also been deposited with the Cambridge Crystallographic Data Centre with the deposition number 831193. These files may be accessed free of charge at http://www.ccdc.cam.ac.uk/conts/retrieving.html.

■ AUTHOR INFORMATION

Corresponding Author

*E-mail: rtpaine@unm.edu.

Notes

The authors declare no competing financial interest.

■ ACKNOWLEDGMENTS

Financial support for this study at the University of New Mexico was provided by the Division of Chemical Sciences, Geosciences and Biosciences, Office of Basic Energy Sciences, U.S. Department of Energy (Grant DE-FG02-03ER15419 (R.T.P)). In addition, funds from the National Science Foundation assisted with the purchases of the X-ray

diffractometer (CHE-0443580) and NMR spectrometers (CHE-0840523 and -0946690). R.T.P. also wishes to thank Dr. Brian M. Rapko for his contributions to the initial stages of this study. B.P.H. and L.H.D. acknowledge support from the Division of Chemical Sciences, Geosciences and Biosciences, Office of Basic Energy Sciences, U.S. Department of Energy. A.d.B.-D. acknowledges financial support from the NSF (CHE-1058805) and Dr. Sebastian Bauer's help with acquisition of the HRMS spectra.

■ REFERENCES

(1) Horwitz, E. P.; Schulz, W. W. *ACS Symp. Ser.* **1999**, *716*, 20−50.

(2) (a) Nash, K. L. *Solvent Extr. Ion Exch.* **1993**, *11*, 729−768. (b) Mathur, J. N.; Murali, M. S.; Nash, K. L. *Solvent Extr. Ion Exch.* **2001**, *19*, 357−390. (c) Nash, K. L. In *Handbook on the Physics and Chemistry of Rare Earths*; Gschneider, K. A., Eyring, L., Jr., Choppin, G. R., Lander, G. H., Eds.; Elsevier Science: Amsterdam, The Netherlands, 1994; Vol. *18*, pp 197−238. (d) Nash, K. L.; Madic, C.; Mathur, J. N.; Lacquement, J. In *The Chemistry of the Actinide and Transactinide Elements*; Morss, L. R., Edelstein, N. M., Fuger, J., Springer: Dordrecht, The Netherlands, 2006; Vol. *4*, Chapter 24, pp 2622−2798. (e) Hill, C. In *Ion Exchange and Solvent Extraction: A Series of Advances*; Moyer, B. A., Ed.; CRC: Boca Raton, FL, 2010; Vol. *19*, pp119−194.

(3) Kolarik, Z. *Chem. Rev.* **2008**, *108*, 4208−4252.

(4) Madic, C.; Lecomte, M.; Baron, P.; Baullis, B. *C. R. Phys.* **2002**, *3*, 797−811.

(5) Dam, H. H.; Reinhaudt, D. N.; Verboom, W. *Chem. Soc. Rev.* **2007**, *36*, 367−377 and references therein.

(6) (a) Ansari, S. A.; Pathak, P.; Mohapatra, P. K.; Mauchand, V. K. *Chem. Rev.* **2012**, *112*, 1751−1772. (b) Ansari, S. A.; Pathak, P.; Mohapatra, P. K.; Mauchand, V. K. *Sep. Purif. Rev.* **2011**, *40*, 43−76. (c) Patil, A. B.; Pathak, P.; Shinde, V. S.; Godbole, S. V.; Mohapatra, P. K. *Dalton Trans.* **2013**, *42*, 1519−1529.

(7) Lewis, F. W.; Hudson, M. J.; Harwood, L. M. *Synlett* **2011**, 2609−2632 and references therein.

(8) (a) Bünzli, J.-C. G. *Acc. Chem. Res.* **2006**, *39*, 53−61. (b) Choppin, G. R.; Jensen, M. P. In *The Chemistry of the Actinide and Transactinide Elements*; Morss, L. R., Edelstein, N. M., Fuger, J., Eds.; Springer: Dordrecht, The Netherlands, 2006; Vol. *4*, Chapter 23, pp 2524−2621. (c) The Lanthanides. In *Comprehensive Inorganic Chemistry*; Pergamon Press: Oxford, 1984; Vol. *4*. (d) The Actinides. In *Comprehensive Inorganic Chemistry*; Pergamon Press: Oxford, 1984; Vol. *5*.

(9) Lehto, J.; Hou, X. *Chemistry and Analysis of Radionuclides*; Wiley-VCH: Weinheim, Germany, 2010.

(10) Flett, D. S. *J. Organomet. Chem.* **2005**, *690*, 2426−2438.

(11) Nilsson, M.; Nash, K. L. *Solvent Extr. Ion Exch.* **2007**, *25*, 665−701.

(12) (a) May, I.; Taylor, R. J.; Denniss, I. S.; Wallwork, A. L. *Czech. J. Phys.* **1999**, *49* (Suppl 1), 597−601. (b) Paiva, A. P.; Malik, P. *J. Radioanal. Nucl. Chem.* **2004**, *261*, 485−496. (c) McKibben, J. M. *Radiochim. Acta* **1984**, *36*, 3−15. (d) Musikas, C.; Schulz, W. W.; Liljenzin, J.-O. In *Solvent Extraction Principles and Practice*, 2nd ed.; Rydberg, J., Cox, M., Musikas, C., Choppin, G., Eds.; Marcel Dekker: New York, 2004; pp 507−557.

(13) (a) Horwitz, E. P.; Kalina, D. G.; Diamond, H.; Vandergrift, G. F.; Schulz, W. W. *Solvent Extr. Ion Exch.* **1985**, *3*, 75−109. (b) Schulz, W. W.; Horwitz, E. P. *Sep. Sci. Technol.* **1988**, *23*, 1191−1210. (c) Horwitz, E. P.; Schulz, W. W. In *The TRUEX Process: A Vital Tool for the Disposal of U.S. Defense Waste*; Elsevier: London, 1991, p 21.

(14) (a) Cuillerdier, C.; Musikas, C.; Hoel, P.; Nigond, L.; Vitart, X. *Sep. Sci. Technol.* **1991**, *26*, 1229−1244. (b) Nigond, L.; Condamines, N.; Cordier, P. Y.; Livet, J.; Madic, C.; Cuillerdier, C.; Musikas, C. *Sep. Sci. Technol.* **1995**, *30*, 2075−2099.

(15) (a) Modolo, G.; Vijgen, H.; Serrano-Purroy, D.; Christiansen, B.; Malmbeck, R.; Sorel, C.; Baron, P. *Sep. Sci. Technol.* **2007**, *42*, 439−452. (b) Modolo, G.; Asp, H.; Schreinemachers, C.; Vijgen, H. *Solvent Extr. Ion Exch.* **2007**, *25*, 703−721. (c) Magnusson, D.; Christiansen, B.; Glatz, J. P.; Malmbeck, R.; Modolo, G. *Solvent Extr. Ion Exch.* **2009**, *27*, 26−35.

(16) (a) Horwitz, E. P.; Kalina, D. G.; Kaplan, L.; Mason, G. W.; Diamond, H. *Sep. Sci. Technol.* **1982**, *17*, 1261−1279. (b) Horwitz, E. P.; Kalina, D. G. *Solvent Extr. Ion Exch.* **1984**, *2*, 179−200. (c) Horwitz, E. P.; Diamond, H.; Martin, K. A.; Chiarizia, R. *Solvent Extr. Ion Exch.* **1987**, *5*, 419−446. (d) Horwitz, E. P.; Diamond, H.; Martin, K. A. *Solvent Extr. Ion Exch.* **1987**, *5*, 447−470. (e) Horwitz, E. P.; Martin, K. A.; Diamond, H.; Kaplan, L. *Solvent Extr. Ion Exch.* **1986**, *4*, 449−494.

(17) (a) Martin, K. A.; Horwitz, E. P.; Ferraro, J. R. *Solvent Extr. Ion Exch.* **1986**, *4*, 1149−1169. (b) Kalina, D. G. *Solvent Extr. Ion Exch.* **1984**, *2*, 381−404.

(18) (a) Bowen, S. M.; Duesler, E. N.; Paine, R. T. *Inorg. Chim. Acta* **1982**, *61*, 155−166. (b) Caudle, L. J.; Duesler, E. N.; Paine, R. T. *Inorg. Chem.* **1985**, *24*, 4441−4444.

(19) Sharova, E. V.; Artyushin, O. I.; Nelyubina, Yu.V.; Lyssenko, K. A.; Passechnik, M. P.; Odinets, I. L. *Russ. Chem. Bull.* **2008**, *57*, 1890−1896.

(20) Boehme, C.; Wipff, G. *Inorg. Chem.* **2002**, *41*, 727−737.

(21) (a) Hay, B. P.; Rustad, J. R.; Hostetler, C. J. *J. Am. Chem. Soc.* **1993**, *115*, 11158−11164. (b) Hay, B. P.; Zhang, D.; Rustad, J. R. *Inorg. Chem.* **1996**, *35*, 2650−2658. (c) Dietz, M. L.; Bond, A. H.; Hay, B. P.; Chiarizia, R.; Huber, V. J.; Herlinger, A. W. *Chem. Commun.* **1999**, 1177−1178. (d) Hay, B. P.; Dixon, D. A.; Vargas, R.; Garza, J.; Raymond, K. N. *Inorg. Chem.* **2001**, *40*, 3922−3935. (e) Lumetta, G. J.; Rapko, B. M.; Garza, P. A.; Hay, B. P.; Gilbertson, R. D.; Weakley, T. J. R.; Hutchison, J. E. *J. Am. Chem. Soc.* **2002**, *124*, 5644−5645. (f) Hay, B. P.; Firman, T. K. *Inorg. Chem.* **2002**, *41*, 5502−5512. (g) Hay, B. P.; Oliferenko, A. A.; Uddin, J.; Zhang, C.; Firman, T. K. *J. Am. Chem. Soc.* **2005**, *127*, 17043−17053. (h) Hay, B. P.; Hancock, R. D. *Coord. Chem. Rev.* **2001**, *212*, 61−78. (i) Parks, B. W.; Gilbertson, R. D.; Hutchison, J. E.; Rather Healy, E.; Weakley, T. J. R.; Rapko, B. M.; Hay, B. P.; Sinkov, S. I.; Broker, G. A.; Rogers, R. D. *Inorg. Chem.* **2006**, *45*, 1498−1507.

(22) (a) Peters, M. W.; Werner, E. J.; Scott, M. J. *Inorg. Chem.* **2002**, *41*, 1707−1716. (b) Matloka, K.; Sah, A. K.; Peters, M. W.; Srinivasan, P.; Gelis, A. V.; Regalbuto, M.; Scott, M. J. *Inorg. Chem.* **2007**, *46*, 10549−10563. (c) Matloka, K.; Sah, A. K.; Srinivasan, P.; Scott, M. J. *C. R. Chim.* **2007**, *10*, 1026−1033.

(23) Reinoso-García, M.; Jańczewski, D.; Reinhoudt, D. N.; Verboom, W.; Malinowska, E.; Pietrzak, M.; Hill, C.; Báĉa, J.; Grüner, B.; Selucky, P.; Grüttner, C. *New J. Chem.* **2006**, *30*, 1480−1492.

(24) Rudzevich, V.; Schollmeyer, D.; Braekers, D.; Desreux, J. F.; Diss, R.; Wipff, G.; Böhmer, V. *J. Org. Chem.* **2005**, *70*, 6027−6033.

(25) Jańczewski, D.; Reinhoudt, D. N.; Verboom, W.; Malinowska, E.; Pietrzak, M.; Hill, C.; Allignol, C. *New J. Chem.* **2007**, *31*, 109−120.

(26) Sharova, E. V.; Artyushin, O. I.; Turanov, A. N.; Karandashev, V. K.; Meshkova, S. B.; Topilova, Z. M.; Odinets, I. L. *Cent. Eur. J. Chem.* **2012**, *10*, 146−156.

(27) (a) Arnaud-Neu, F.; Böhmer, V.; Dozol, J.-F.; Grüttner, C.; Jakobi, R. A.; Kraft, D.; Mauprivez, O.; Rouquette, H.; Schwing-Weill, M.-J.; Simon, N.; Vogt, W. *J. Chem. Soc., Perkin Trans.* **1996**, *2*, 1175−1182. (b) Delmau, L. H.; Simon, N.; Schwing-Weill, M.-J.; Arnaud-Neu, F.; Dozol, J.-F.; Eymard, S.; Tournois, B.; Böhmer, V.; Grüttner, C.; Musigmann, C.; Tunayar, A. *J. Chem. Soc., Chem. Commun.* **1998**, 1627−1628. (c) Delmau, L. H.; Simon, N.; Schwing-Weill, M.-J.; Arnaud-Neu, F.; Dozol, J.-F.; Eymard, S.; Tournois, B.; Grüttner, C.; Musigmann, C.; Tunayar, A.; Böhmer, V. *Sep. Sci. Technol.* **1999**, *34*, 863−876. (d) Arduini, A.; Böhmer, V.; Delmau, L. H.; Desreux, J.-F.; Dozol, J.-F.; Garcia Carrera, M. A.; Lambert, B.; Musigmann, C.; Pochini, A.; Shivanyak, A.; Ugozzoli, F. *Chem.—Eur. J.* **2000**, *6*, 2135−2144. (e) Lambert, B.; Jacques, V.; Shivanyuk, A.; Matthews, S. E.; Tunayar, A.; Baaden, M.; Wipff, G.; Böhmer, V.; Desreux, J. F. *Inorg. Chem.* **2000**, *39*, 2033−2041. (f) Arnaud-Neu, F.; Barboso, S.; Böhmer, V.; Brisach, F.; Delmau, L. H.; Dozol, J.-F.; Mogck, O.; Paulus, E. F.; Saadioui, M.; Shivanyak, A. *Aust. J. Chem.* **2003**, *56*, 1113−1119. (g) Babain, V. A.; Alyapyshev, M. Yu.; Karavan, M. D.; Böhmer, V.; Wang, L.; Shokova, E. A.; Motornaya, A. E.; Vatsouro, I.

M.; Kovalev, V. V. *Radiochim. Acta* **2005**, *93*, 749−756. (h) Motornaya, A.; Vatsouro, I.; Shokova, E.; Hubscher-Bruder, V.; Alyapyshev, M.; Babain, V.; Karavan, M.; Arnaud-Neu, F.; Böhmer, V.; Kovalev, V. *Tetrahedron* **2007**, *63*, 4748−4755. (i) Peters, C.; Braekers, D.; Kroupa, J.; Kasyan, O.; Miroshnichenko, S.; Rudzevich, V.; Böhmer, V. *Radiochim. Acta* **2008**, *96*, 203−210. (j) Sansone, F.; Galletta, M.; Macerata, E.; Trivellone, E.; Giola, M.; Ungaro, R.; Böhmer, V.; Casnati, A.; Mariani. *Radiochim. Acta* **2008**, *96*, 235−239. (k) Dordea, C.; Brisach, F.; Haddaoui, J.; Arnaud-Neu, F.; Bolte, M.; Casnati, A.; Böhmer, V. *Supramol. Chem.* **2010**, *22*, 347−357. (l) Vatsouro, I.; Serebryannikova, A.; Wang, L.; Hubscher-Bruder, V.; Shokova, E.; Bolte, M.; Arnaud-Neu, F.; Böhmer, V.; Kovalev, V. *Tetrahedron* **2011**, *67*, 8092−8101.

(28) (a) Boerrigter, H.; Verboom, W.; Reinhoudt, D. N. *J. Org. Chem.* **1997**, *62*, 7148−7155. (b) Boerrigter, H.; Verboom, W.; Reinhoudt, D. N. *Liebigs Ann./Recl.* **1997**, 2247−2254.

(29) Arnaud-Neu, F.; Barboso, S.; Byrne, D.; Charbonniere, L. J.; Schwing-Weill, M. J.; Ulrich, G. In *Calixarenes for Separations*; Lumetta, G. J., Rogers, R. D., Gopalan, A. S., Eds.; American Chemical Society: Washington, DC, 2000; p 150.

(30) (a) McCabe, D. J.; Russell, A. A.; Karthikeyan, S.; Paine, R. T.; Ryan, R. R.; Smith, B. *Inorg. Chem.* **1987**, *26*, 1230−1235. (b) Conary, G. S.; Russell, A. A.; Paine, R. T.; Hall, J. H.; Ryan, R. R. *Inorg. Chem.* **1988**, *27*, 3242−3245. (c) Russell, A. A.; Meline, R. L.; Duesler, E. N.; Paine, R. T. *Inorg. Chim. Acta* **1995**, *231*, 1−5.

(31) (a) Rapko, B. M.; Duesler, E. N.; Smith, P. H.; Paine, R. T.; Ryan, R. R. *Inorg. Chem.* **1993**, *32*, 2164−2174. (b) Engelhardt, U.; Rapko, B. M.; Duesler, E. N.; Frutos, D.; Paine, R. T. *Polyhedron* **1995**, *14*, 2361−2369. (c) Bond, E. M.; Gan, X.; FitzPatrick, J. R.; Paine, R. T. *J. Alloys Compd.* **1998**, *271*−*273*, 172−175. (d) Bond, E. M.; Duesler, E. N.; Paine, R. T.; Neu, M. P.; Matonic, J. H.; Scott, B. L. *Inorg. Chem.* **2000**, *39*, 4152−4155. (e) Bond, E. M.; Duesler, E. N.; Paine, R. T.; Nöth, H. *Polyhedron* **2000**, *19*, 2135−2140. (f) Gan, X.-M.; Parveen, S.; Smith, W. L.; Duesler, E. N.; Paine, R. T. *Inorg. Chem.* **2000**, *39*, 4591−4598. (g) Matonic, J. H.; Neu, M. P.; Enriquez, A. E. *J. Chem. Soc., Dalton Trans.* **2002**, 2328−2332. (h) Gan, X.-M.; Duesler, E. N.; Paine, R. T. *Inorg. Chem.* **2001**, *40*, 4420−4427. (i) Matonic, J. H.; Enriquez, A. E.; Scott, B. L.; Paine, R. T.; Neu, M. P. *Nucl. Sci. Technol.* **2002**, *3*, 100−105. (j) Paine, R. T.; Bond, R. T.; Bond, E. M.; Parveen, S.; Donhart, N.; Duesler, E. N.; Smith, K. A.; Nöth, H. *Inorg. Chem.* **2002**, *41*, 444−448. (k) Gan, X.-M.; Paine, R. T.; Duesler, E. N.; Nöth, H. *Dalton Trans.* **2003**, 153−159. (l) Gan, X.-M.; Rapko, B. M.; Duesler, E. N.; Binyamin, I.; Paine, R. T.; Hay, B. P. *Polyhedron* **2005**, *24*, 469−474. (m) Pailloux, S.; Shirima, C. E.; Ray, A. D.; Duesler, E. N.; Paine, R. T.; Klaehn, J. R.; McIlwain, M. E.; Hay, B. P. *Inorg. Chem.* **2009**, *48*, 3104−3113. (n) Pailloux, S.; Shirima, C. E.; Ray, A. D.; Duesler, E. N.; Smith, K. A.; Paine, R. T.; Klaehn, J. R.; McIlwain, M. E.; Hay, B. P. *Dalton Trans.* **2009**, 7486−7493.

(32) Bond, E. M.; Engelhardt, U.; Deere, T. P.; Rapko, B. M.; Paine, R. T. *Solvent Extr. Ion Exch.* **1997**, *15*, 381−400.

(33) Bond, E. M.; Engelhardt, U.; Deere, T. P.; Rapko, B. M.; Paine, R. T. *Solvent. Extr. Ion Exch.* **1998**, *16*, 967−983.

(34) Nash, K. L.; Lavallette, C.; Borkowski, M.; Paine, R. T.; Gan, X.-M. *Inorg. Chem.* **2002**, *41*, 5849−5858.

(35) Sulakova, J.; Paine, R. T.; Chakravarty, M.; Nash, K. L. *Sep. Sci. Technol.* **2012**, *47*, 1−9.

(36) The atom numbering systems employed for the NMR chemical shift assignments are given in the Supporting Information.

(37) Samples of 2-(diphenylphosphinoylmethyl)pyridine can be efficiently prepared by chloride substitution on 2-(chloromethyl) pyridine by using either $K[PPh_2]$ followed by oxidation[31a] or the phosphinoyl methyl Grignard reagent, $[Ph_2P(O)CH_2]Mg$, prepared as described for analogous reagents.[31n,34]

(38) (a) Caudle, L. J.; Duesler, E, N; Paine, R. T. *Inorg. Chim. Acta* **1985**, *110*, 91−100. (b) Caudle, L. J. Ph.D. Thesis, University of New Mexico, 1983.

(39) (a) Baker, W.; Buggle, K. M.; McOmie, J. F. W.; Watkins, D. A. M. *J. Chem. Soc.* **1958**, 3594−3603. (b) Sakata, K.; Ueno, A. *Synth. React. Inorg. Met.-Org. Chem.* **1991**, *21*, 729−739.

(40) Horrocks, W. D., Jr.; Sudnick, D. R. *Acc. Chem. Res.* **1981**, *14*, 384−392.

(41) *APEX 2*; Bruker AXS, Inc.: Madison, WI, 2007. (b) *SAINT+ 7.01*; Bruker AXS, Inc.: Madison, WI, 2003. (c) Sheldrick, G. M.*SADABS 2.10*; University of Gottingen: Gottingen, Germany, 2003.

(42) *SHELXL-97*; Bruker AXS, Inc.: Madison, WI, 2008.

(43) (a) van der Sluis, P.; Spek, A. L. *Acta Crystallogr.* **1990**, *A46*, 194−201. (b) Spek, A. L. *Acta Crystallogr.* **1990**, *A46*, C34.

(44) (a) Allinger, N. L.; Yuh, Y.-H.; Lii, J.-H. *J. Am. Chem. Soc.* **1989**, *111*, 8551−8566. (b) Lii, J.-H.; Allinger, N. L. *J. Am. Chem. Soc.* **1989**, *111*, 8566−8575. (c) Lii, J.-H.; Allinger, N. L. *J. Am. Chem. Soc.* **1989**, *111*, 8576−8582.

(45) Hay, B. P. *Coord. Chem. Rev.* **1993**, *126*, 177−236.

(46) *PCModel, version 9.3*; Serena Software: Bloomington, Indiana.

(47) An X-ray structure determination for a second crystal of **9** revealed the *S,S* enantiomer. The data are included in the Supporting Information.

(48) Antipin, M. Yu; Struchkov, Yu. T.; Matrosov, E. I.; Kabachnik, M. I. *J. Struct. Chem.* **1985**, *26*, 441−446.

(49) An X-ray structure determination for a second crystal obtained by crystallization of a sample of **8** by slow diffusion of isopropyl ether vapor through a EtOAc solution of the racemic mixture contained both *R* and *S* enantiomers.

(50) (a) *Cambridge Structural Database, Version 5.33*; November 2011. (b) Allen, F. H. *Acta Crystallogr., Sect. B.* **2002**, *B58*, 380−388. (c) Bruno, I. J.; Cole, J. C.; Edgington, P. R.; Kessler, M.; Macrae, C. F.; McCabe, P.; Pearson, J.; Taylor, R. *Acta Crystallogr., Sect. B* **2002**, *B58*, 389−397.

(51) (a) Cotton, F. A. *Chemical Applications of Group Theory*, 2nd ed.; Wiley-Interscience: New York, 1963. (b) Tanner, P. A. Lanthanide Luminescence in Solids. In *Lanthanide Luminenscence: Photophysical, Analytical and Biological Aspects*; Hänninen, P., Härma, H., Eds.; Springer Series in Fluorescence, 2011; Vol. *7*, pp 183−234.

(52) In these initial extraction characterization studies, quantitative determinations of nitric acid extraction by the free ligands in DCE have not been performed. On the basis of prior studies of the protonation equilbria of TONOPOPO in toluene with HNO_3,[35]it is expected that the corrections to the ligand:metal ion equilibria will not be large especially for **9**. These measurements and nitrate dependency studies will be undertaken in the near future with derivatives of **9** and **10** that are soluble in dodecane solutions.